journal of the international meteor organization

WGN

45:2
april 2017

Group observations by Japanese students
Diurnal variation in meteor flux from radio data
Confirmation of June Theta-Serpentids
October–November video meteors

ISSN 1016-3115

WGN Vol. 45, No. 2, April 2017, pp. 25 – 46

Administrative

Meteor science

Short communication

Preliminary results

Front cover photo

Spectacular fireball photographed from Waldzell, Oberösterreich, Austria on 2017 March 25 at $23^{h}35^{m}$ UT. Photo courtesy: Christian Koll.

Writing for WGN

This Journal welcomes papers submitted for publication. All papers are reviewed for scientific content, and edited for English and style. Instructions for authors can be found in WGN **31:4**, 124–128, and at `http://www.imo.net/docs/writingforwgn.pdf` .

Legal address

International Meteor Organization, Jozef Mattheessensstraat 60, 2540 Hove, Belgium.

Letter — Entertaining meteor observations by a student group — 2016 Perseids by Meiji University students

Masahiro Koseki[1], *Yoshihiko Shigeno*[2], *Tatsuya Hiraizumi*[3]

It seems group observing of meteors is not approved today. Aren't the results of group observing useful? In our opinion the answer is yes, group observing is entertaining and bears fruits well even if their first observation. We show group observing by students can yield comparable results to veteran observer's and, more, students are encouraged to do further studies.

We examined the reports of Meiji University students including their first meteor observations and get reasonable ZHRs and the magnitude ratios. It is suggested even chats during observations could stir up their morale and they learn how to observe meteors in practice. This report is an answer from Japan for 'A perspective on the future of meteor astronomy' discussed in IMO members.

1 Observations

Members of Meiji University Astronomical Club made an expedition for 2016 Perseids and stayed at Aizu Astraea Lodge in Minami-Aizu heights Fukushima during 2016 August 10–16 (Figure 1). The list below shows the participants of observations including those that are not meteor section members. Almost all freshmen experienced their first meteor observations and many others also are not trained in it.

Figure 1 – Meiji University 2016 Perseids campaign participants.

They organized two teams of six for each time span; recorder, time keeper and four observers each. They seated as shown in Figure 2 and two teams depart 10–15 m apart. When a meteor appeared, observers call meteor magnitude and shower membership. Figure 3 shows a recoding sheet for an example.

They could observe Perseids only two nights August 11/12 and 12/13. Their Perseids campaign by the style shown below has started since 2010 but resulted in failure three times 2011, 2014 and 2015, because summer season in Japan is wet. Many Japanese observers were hindered by bad weather and by the existence of the moon in evening sky 2016. They were even lucky in Japanese circumstances last year and enjoyed Perseids display of bright meteors. Table 1 presents the summary results.

[1] 4-3-5 Annnaka Annaka-shi, Gunma-ken, 379-0116, Japan. The Nippon Meteor Society (NMS). Email: geh04301@nifty.ne.jp
[2] 5-6 Kizuki-Sumiyoshi, Kawasaki City, 211-0021, Japan. Meteor Science Seminar (MSS). Email: cyg@msswg.net
[3] 4-3-18 Nishinogawa, Komae City, Tokyo, 201-0001, Japan. Meiji University Astronomical Club.
Email: libra.h.tty.104@gmail.com

Table 1 – Summary results of Perseids campaign 2016. Lm with an asterisk represents observations under moonlight. Slashes in the duration columns show two groups started/ended observations independently and the duration differs.

Day	Time	Duration	Perseids			Sporadics			Lm
		(min)	N	HR	Sum	N	HR	Sum	
11/12	21	40/43	2 ∼ 5	2.8 ∼ 7.5	24	0 ∼ 5	0 ∼ 7.5	21	2.89 ∼ 4.67*
	22	50	3 ∼ 10	3.6 ∼ 12.0	48	4 ∼ 10	4.8 ∼ 12.0	52	2.89 ∼ 4.67*
	23	50	7 ∼ 17	8.4 ∼ 20.4	94	4 ∼ 14	4.8 ∼ 16.8	66	2.89 ∼ 5.08
	00	45/49	5 ∼ 18	6.7 ∼ 22.0	82	4 ∼ 13	4.9 ∼ 17.3	74	4.66 ∼ 5.80
	01	52	9 ∼ 15	10.4 ∼ 17.3	50	13 ∼ 34	15.0 ∼ 39.2	88	5.08 ∼ 5.49
	02	45/49	11 ∼ 21	13.5 ∼ 28.0	127	6 ∼ 26	8.0 ∼ 31.8	112	2.84 ∼ 5.56
	03	54	9 ∼ 13	10.0 ∼ 14.4	45	6 ∼ 11	6.7 ∼ 12.2	32	5.49
12/13	21	30/35	1 ∼ 6	2.0 ∼ 10.3	21	2 ∼ 8	4.0 ∼ 13.7	36	2.89*
	22	35/50	7 ∼ 12	8.4 ∼ 18.9	73	4 ∼ 17	4.8 ∼ 29.1	70	2.89 ∼ 5.08*
	23	50/55	8 ∼ 20	8.7 ∼ 24.0	99	3 ∼ 10	3.6 ∼ 10.9	48	4.66 ∼ 5.08
	01	54	28 ∼ 31	31.1 ∼ 34.4	120	16 ∼ 25	17.8 ∼ 27.8	84	5.08 ∼ 5.56
	02	50/60	15 ∼ 26	16.0 ∼ 31.2	174	6 ∼ 17	7.0 ∼ 18.0	100	5.08 ∼ 5.80
Total		3984			957			783	

The participants of 2016 Perseids campaign in Aizu were as follows:

Freshman: Kazuki Aigo, Miyuki Aoyama, Tatsuki Ashida, Hikaru Izhima, Miwa Ichikawa, Erika Imai, Kentaro Okuma, Nagisa Okazhima, Sho Osano, Momomi Kimmura, Kosei Kataoka, Ryota Kudo, Akane Kuwakubo, Ikuya Satake, Takumi Sato, Kaina Shibata, Mihoko Suzuki, Kota Tanikawa, Koki Tsuda, Kaho Nagata, Shiyu Nakamura, Atsuya Nimi, Nobutaka Niwa, Rintaro Noda, Wataru Hayasaka, Tichi Hirabayashi, Tomoaki Fujita, Yudai Hojo, Atsuko Matsumoto, Hirohiko Mizuno, Yuki Yamahash, Tichi Yokoe.

Sophomore: Atsushi Owada, Yu Ozawa, Soichiro Kato, Daiki Kimiduka, Tomohiro Kuno, Naoto Koyama, Takaya Saito, Akari Sakanashi, Shoseki, Kazuki Sugi, Yugo Tokino, Ryo Nagasawa, Ozora Nobata, Takumi Haba, Tatsuya Hiraizumi, Ryo Moriya, Shuhei Yamakawa, Daiki Yonemochi.

Junior: Nanako Abe, Saki Izawa, Kazuki Ide, Yu Iwase, Mayu Ueda, Yuka Utsumi, Rika Oki, Azumi Ono, Mami Kawai, Maho Kawakami, Shino Kimura, Reo Kotani, Maho Sasaki, Natsumi Suzuki, Ryota Suzuki, Hiroko Sone, Masono Takshima, Naoyuki Takahashi, Takayuki Teramura, Keita Nawata, Anna Niwa, Seiichiro Hagino, Natsumi Yoshida, Mitsfumi Yoshimura.

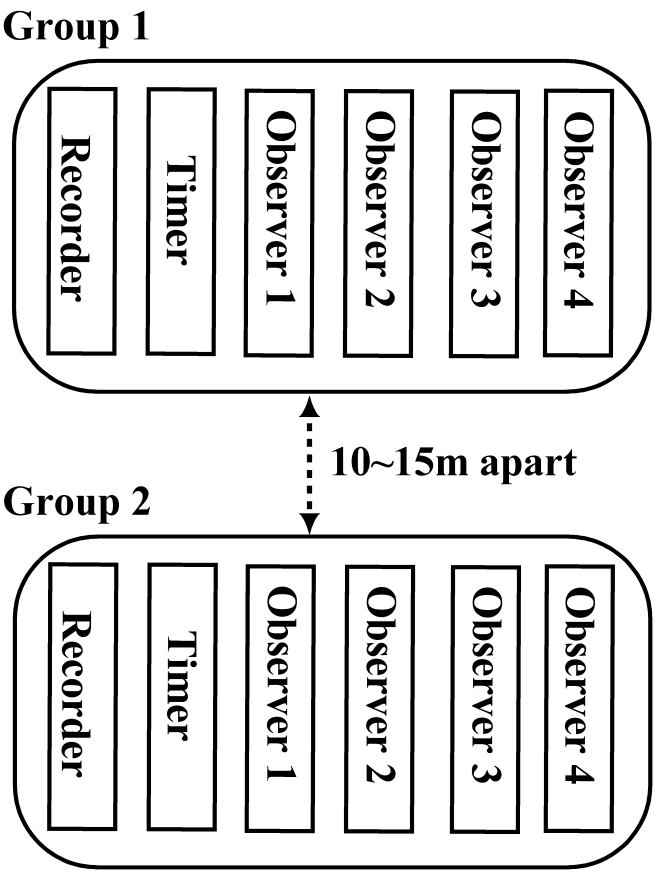

Figure 2 – The disposition of 2016 Perseids campaign.

2 Results from observations

2.1 ZHRs

Observations in evening hours were hindered much by moonlight and the limiting magnitude records are wide spread (Table 1). If we calculate ZHRs strictly by the records, they would reach unreliable values. It is necessary to correct the record by the method described in following section (3.1 Limiting magnitude) and, then, we get proper results as shown in Figure 4.

2.2 Magnitude ratio

If we corrected the observed limiting magnitude by following way (3.1 Limiting magnitude), we could get good estimates of the magnitude ratio of Perseids also. There are two ways to estimate the magnitude ratio; compensating the observed limiting magnitude to the ideal sky by Kresáková's (1966) perception coefficient or comparing magnitude distribution with sporadic one (see 2.2.2).

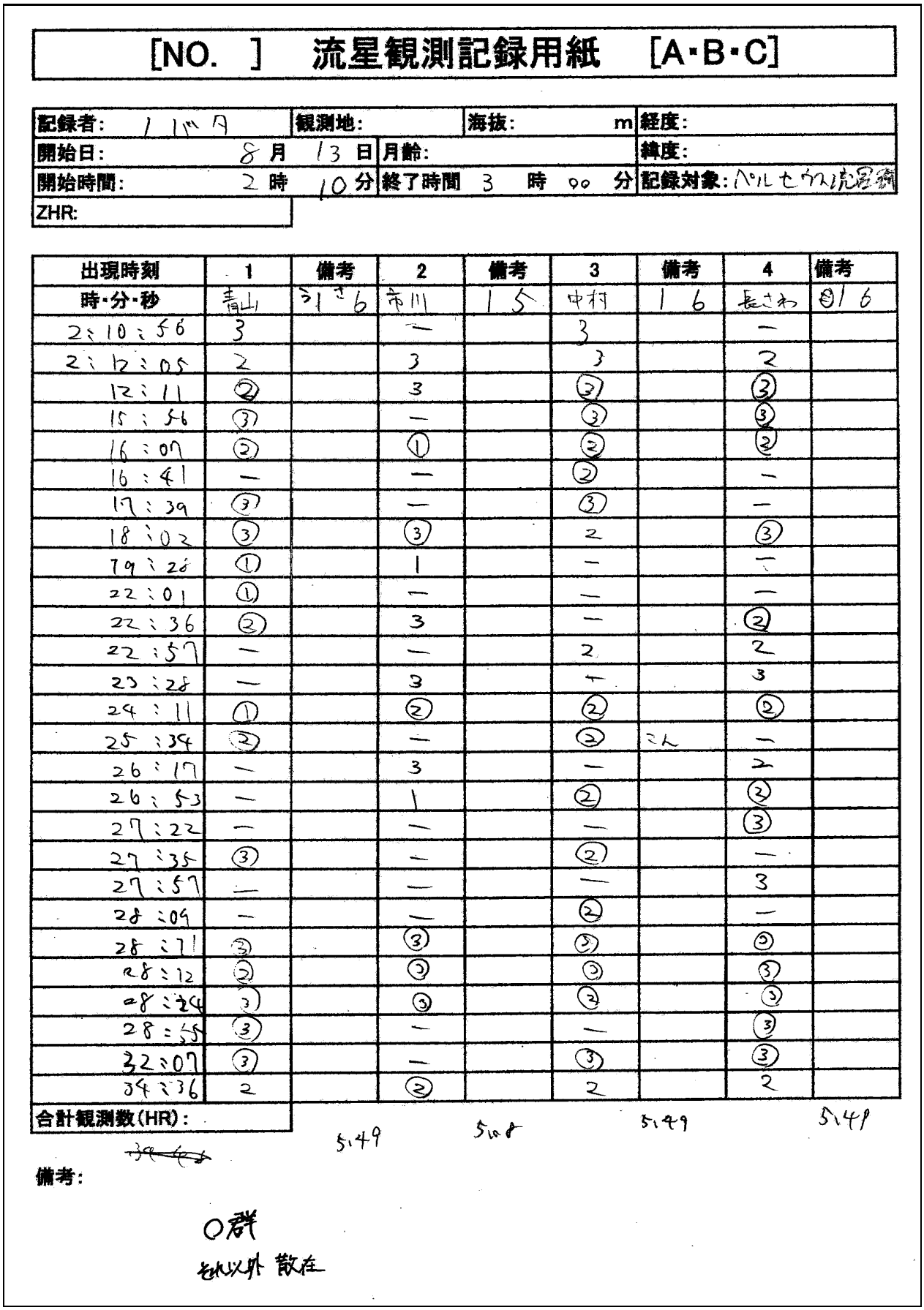

[NO.] 流星観測記録用紙 [A・B・C]

記録者: 1 1ばん	観測地:	海抜: m	経度:
開始日: 8 月 13 日	月齢:		緯度:
開始時間: 2 時 10 分	終了時間 3 時 00 分		記録対象: ペルセウス流星群
ZHR:			

出現時刻	1	備考	2	備考	3	備考	4	備考
時・分・秒	青山	51 6	市川	15	中村	16	長さわ	8/16
2:10:56	3		—		3		—	
2:12:05	2		3		3		2	
12:11	②		3		②		③	
15:56	③		—		③		③	
16:09	②		①		②		②	
16:41	—		—		②		—	
17:39	③		—		③		—	
18:02	③		③		2		③	
19:26	①		1		—		—	
22:01	①		—		—		—	
22:36	②		3		—		②	
22:57	—		—		2		2	
23:28	—		3		—		3	
24:11	①		②		②		②	
25:34	②		—		②	こん	—	
26:17	—		3		—		2	
26:53	—		1		②		②	
27:22	—		—		—		③	
27:35	③		—		②		—	
27:57	—		—		—		3	
28:09	—		—		②		—	
28:11	③		③		③		③	
28:12	②		③		③		③	
28:24	③		③		②		③	
28:55	③		—		—		③	
32:07	③		—		③		③	
34:36	2		②		2		2	
合計観測数(HR):								
	~~39 4~~		5.49	5.08		5.49		5.49

備考:

○群

それ以外 散在

Figure 3 – An example of the recording sheet of group observing. The first frame; Title, the second; Primary observational records (Day, time, location, and so on.), the third; records for individual meteors (four observers' magnitude estimates are shown in each column with indication for Perseids by a circle.).

2.2.1 Compensating by Kresáková's perception coefficient

We calculate ZHRs by the formula such as ZHR = $\mathrm{HR}r^{m-m_0}/\sin h$, where HR is the hourly meteor rates, r is the magnitude ratio, m is the observed limiting magnitude (Lm) and m_0 is set 6.5 usually. Here we accept the hypothesis that we might see meteors in proportion to the power of the difference between m and m_0. This means we consider the perception coefficient would be shifted by the difference between m and m_0 also.

One of the author, Koseki (2011) modified Kresáková's table to 0.1 magnitude bin interpolating with the third power function. We use the modified table to compensate the meteor number and estimate the magnitude ratios for Perseids and sporadics (see for an example Figure 5). We can estimate the magnitude ratios from the slope of the drawn in the figure for Perseids and sporadics $r_{\mathrm{Per}} = 2.11$ and $r_{\mathrm{spo}} = 3.15$ respectively.

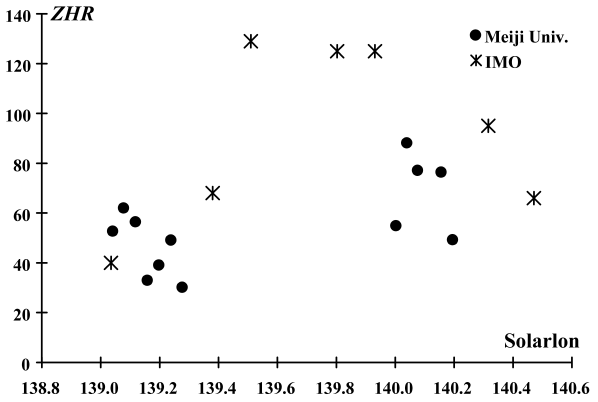

Figure 4 – ZHRs calculated from students' observation (black circle) comparing with IMO VMDB (2016, asterisk).

2.2.2 Comparing meteor numbers of Perseids with sporadics

If we assumed the perception coefficient of Perseids equals to sporadics, we could calculate the ratios of Perseids to sporadics not using any supposed perception coefficient. Figure 6 gives an example from the same observation period of Figure 5. If we use $r_{\mathrm{spo}} = 3.5$ based on Kresáková's result, we could estimate $r_{\mathrm{Per}} = 2.14$ from the slope of the line.

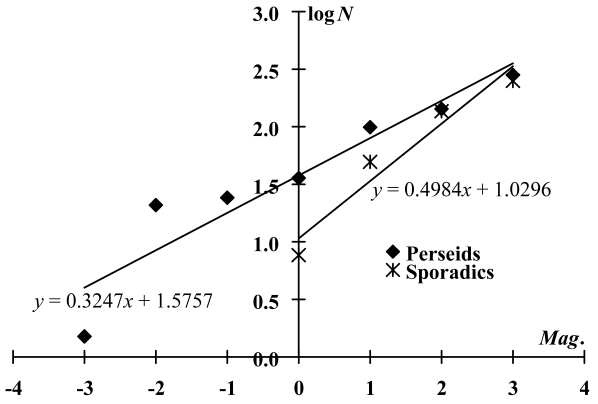

Figure 5 – Magnitude distributions of Perseids and sporadics compensated by Kresakova's perception coefficient (modified). Data used here are combined two groups of 12/13 night 23 JST period.

3 Problems

3.1 Limiting magnitude

As shown in Table 1 the observed limiting magnitudes (Lm) differ very widely because of the disturbance of the moonlight and of inexperience of observers to such recording. IMO instructs to select the area in which star number increases smoothly near Lm in order to record Lm correctly. But, sometimes we need observations of major meteor showers when the moon is bright or when city light hinders much. In such cases, we cannot help using discontent areas and are confronted with a difficult problem to estimate proper Lm.

We have two approaches to reach reasonable Lm; the meteor magnitude distribution and the existence of two independent observing groups in this case.

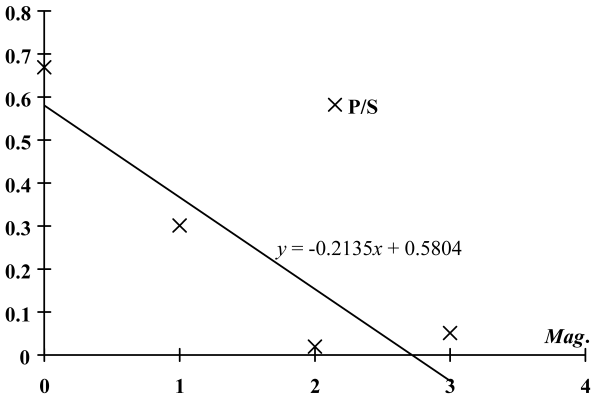

Figure 6 – Perseid meteor ratios to sporadics with magnitudes.

Firstly, we test observed magnitude distribution and Lm by shifting Kresáková's perception coefficient at where we could get the proper magnitude ratio. Table 2 lists the magnitude distribution of 8 observers (see the second line of Table 1). It is clear they could not recognize magnitude +3 meteors and magnitude ratios both Perseids and sporadics would be reached improbable value if Lm = 2.89 is correct. If we shifted supposed Lm to 4.7 on the basis of an observer's report Lm = 4.67, we could get $r_{\mathrm{Per}} = 3.01$, $r_{\mathrm{spo}} = 3.76$. It is suggested we can select the faintest Lm in all reports or the next star in Lm table rather than reported value themselves. This suggestion can be confirmed by following interesting observations.

Secondly, we compare the report of two groups apart 10–15 m, who recorded Lm independently by using different areas in 12/13 night 22 JST period. One used No. 6 and other No. 16. Former group recorded Lm = 2.89, because they hindered much by moonlight and could see only corner stars. Another turn opposite to the moon and got Lm = 4.66–5.08. Nevertheless, two groups observed similar sky area, that is, up to the zenith. Therefore,

Table 2 – The magnitude distribution in the moonlight.

Date	JST	mag.	0	+1	+2	+3
11/12	21:17(20)–22:00	Perseids	0	10	11	3
		Sporadics	0	2	15	4

we can combine two observations and test above suggestion. Figure 7 shows clearly the estimation of Lm = 5.08 is better than Lm = 2.89; the estimated magnitude distribution by shifting Kresáková's perception coefficient to Lm = 5.1 (Perseids_Lm = 5.1 in Figure 7) seems to be more probable than Lm = 3.5. We would be better to use 'next' star in the Lm tables to the reported Lm (star) itself when the sky condition is not good. We get ZHRs in the section 2.1 ZHRs by this manner.

3.2 Membership judgement

Though we can get proper magnitude ratios for Perseids and sporadics in 2.2.1., there are several cases which show unreliable meteor number ratio Perseids to sporadics and give the contrary magnitude ratios. 11/12 night 01 JST period is an example; $N_{\mathrm{Per}}/N_{\mathrm{spo}} = 50/88$, $r_{\mathrm{Per}} = 3.36$ and $r_{\mathrm{spo}} = 2.02$. Koseki (2011) pointed out beginners intend to reject possible Perseids out to sporadics. When a beginner looks up the zenith heading for the south, he/she would see meteors distant from the radiant point and feel difficulty to classify them as Perseids/sporadics. We had better note Perseids magnitude ratios from whole data in this campaign might be higher than the real one and ZHRs lower. But, if we choose carefully observations done properly, we could get very nice results shown in 2.2.1.

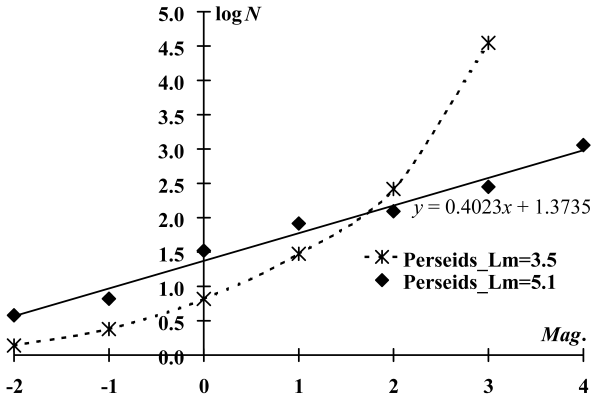

Figure 7 – Comparison with the compensation of the limiting magnitude on the magnitude distribution.

3.3 Magnitude estimation

Some groups have a tendency to estimate meteor magnitude narrower extent. It may be suggested they are not familiar with a fireball and to record faint meteors and record them moderate magnitude. But, as Figure 8 shows a good linear expression, they had done good job for estimating meteor magnitude. Shigeno and Toda (2008) concluded that mean magnitude estimates by students equals of video ones.

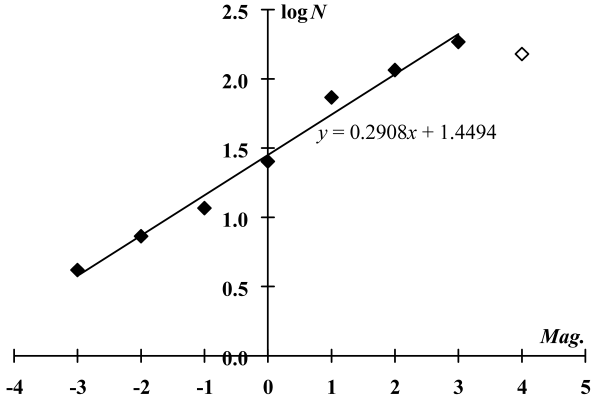

Figure 8 – Magnitude distribution compensated by Kresakova's perception coefficient (modified). Data used here are 12/13 night whole records and the magnitude distributions of each period are weighted by each Perseids number.

4 Discussions

Japanese meteor observers have discussed the future meteor observations with several IMO members and it became clear that encouraging young observers is very important. This report is an answer from Japan and following discussions are based on such progress. The outline of this report was presented at the 145th MSS (Meteor Science Seminar) meeting and we exchanged the ideas for enjoying observations and obtaining more useful results.

Determination of the limiting magnitude is difficult for every observer. We feel uncertain the faintest star we look is real one or a vision. It is recommended we accept such star as real or we estimate the limiting magnitude from the next star we confirm.
→ Students are not familiar with any asterisms always and they missed area No.14 which is the most suitable in their observations in this campaign.

The bulk data from student group observing make possible to reach reliable results, though each data might be insufficient, that is, errors of the identification and estimates of magnitude exist somewhere.
+ Student observations must be entertaining and this leads to gather more and more participants.
→ Checks of the data are necessary. It should be corrected the limiting magnitude report by comparing magnitude distributions of observations with estimates from the perception coefficient for an example.

There may be interference between observers when they seat near and call their estimates to a recorder, but such conversations or even chats play important role in group observing especially for students.
+ Chats keep one awake.
+ If one slipped a meteor, he/she would concentrate his/her care to the sky not to overlook the next.
+ If estimates were different, they might talk about it and make efforts to get more proper results.

Observers in this campaign saw the same area but it seems to be interesting to see different areas. They may count different meteor number.
+ The group observing is said to do so as Levy (2008) wrote.
+ It would be useful to observe 90 degrees different direction each four members.
→ Observers who see the opposite direction to the radiant might feel difficulties to classifying meteors.
+ It would be entertaining and interesting to alter the center of one's view; who could count meteors most?
→ It is necessary to special chair to alter one's view or a "coffin". If not, the change from the zenith could not be larger than 30 degrees.
→ To look the same view and to chat on the event are joyful and give useful experiences for students.

It is very useful to keep looking up the sky and record meteors on a roll paper not looking down the record.
+ A recorder and a time keeper can join observations. Time calling might be left to a talkative clock.
→ Chattering with neighbor observers is useful to activate observers' mind.

We feel happy when we take a meal together and would take a positive attitude (Figure 9).
→ To avoid being sleepy in observations, we had better be careful in overeating or enjoying alcohol drinks.

Figure 9 – Joy of the expedition: students powered by meals.

The observational method might be different with what is the goal of observations.
+ Observers seat side by side and call witness to a recorder when we intend to enjoy and skill up observations.
+ Observers seat radially and write down record by oneself when we try to get better results.
→ This method is good for veteran observers not for students.
+ Experienced and enthusiastic students can challenge video, radio observations simultaneously with visual ones.

Group observing sheets (Figure 3) give more information for future meteor works.
+ We can study why the difference magnitude estimates causes; the existence of the train, the angular speed of a meteor (the distance from the radiant in case of a meteor shower), and etc.
+ The rate of missed meteors with magnitude could give us real perception coefficients.
+ The relation of the rate of different classification to the distance from the radiant might suggest us the ideal direction of the center of the view.
→ IMO instructs us to see the areas distant from the radiant 20–40 degrees. It is a good idea all four observers faces to such area but it is problematic to post one who see the unfavorable direction when they turn to different direction.

[NOTE]: Why Japanese observers often look up the zenith?

Light pollutions became severe in the last quarter of the 20th century in Japan and many observers looked up the zenith in order to avoid poor sky. To observe zenith area is said as the ordinary way in visual observations even if the good sky condition afterward. Many observers now record meteor numbers and magnitude estimates only, not plotting meteor paths on the charts and, so, it is easier to lie on a rug than sit on a chair. Guidance books recommend beginners to look up the zenith and young observers act in obedience to the instruction, though skilled observers view where they like, of course.

References

IMO VMDB (2016). "Perseids 2016 campaign". `http://www.imo.net/members/imo_live_shower?shower=PER&year=2016` .

Koseki M. (2011). "An analysis of visual group observing by Meiji University students: 2010 Perseids". (presented in 127th MSS meeting (in Japanese).).

Kresáková M. (1966). "The magnitude distribution of meteors in meteor streams". *Contr. astron. obs. Skalnate Pleso*, pages 75–109.

Levy D. H. (2008). *David Levy's Guide to Observing Meteor Showers*. Cambridge.

Shigeno Y. and Toda M. (2008). "Comparison of TV magnitudes and visual magnitudes of meteors". *WGN, Journal of the International Meteor Organization*, **36:4**, 79–82.

IMO bibcode WGN-452-koseki-letter NASA-ADS bibcode 2017JIMO...45...25K

Call for photographs

Javor Kac

We are frequently short of photographs for the *WGN* covers that we publish in colour (front cover) or black&white (back cover). If you think you have a suitable meteor-related photograph, please offer it to us. More or less any computer image format will do. You can send your photographs to `wgn@imo.net`, but remember to put 'Meteor' in the subject line to get round the anti-spam filters.

IMO bibcode WGN-452-kac-call NASA-ADS bibcode 2017JIMO...45...31K

Meteor science

Modelling & analysis of diurnal variation in meteor flux

C. Powell[1,2,3]

Temporal and spatial variations of peak hour and idealised sine function fit are considered in reflection of an extended model of the diurnal shift mechanism. This model is formed by extension of the currently understood mechanism, providing a mathematical argument focusing on orbital velocity. Hourly detection counts collected by forward-scatter radio detection are used as data to analyse the form of diurnal shift for each observer. The fit and mean peak hour of the diurnal shift and are considered across nearly 350 observers, analysing variation from 2000 to 2016, as well as variation between data from 9 latitude and 14 longitude categories spanning at most 10° each, to determine the agreement of data with the model. Modelling the orbital velocity of Earth as a primary factor behind diurnal variation is supported by the timezone corrected peak hours and correlation with longitude. The mechanism does not appear to vary with time, however the relative intensity of diurnal variation with respect to background detection counts is damped as a maximum in these hourly detection counts is observed. This provides a mathematical model of the diurnal shift mechanism, accompanied with support from a large dataset.

Received 2017 March 22

1 Introduction

Diurnal variation, a notable increase and decrease in meteor flux over the time scale of a single day, has been observed and studied previously; observations are frequently reported, for example Kero et al. (2012) and Okamoto & Maegawa (2008). It is known that the variation relies on the rotation of Earth altering the component of orbital velocity contributing to a meteor's incident velocity. However, this has not been described in any mathematical detail. The motivation for this article is the formulation of a model describing the mechanism that causes diurnal variation, and subsequent comparison against data.

In order to compare the model to the data, a collection of hourly detection counts provided by forward-scatter radio detection is used to examine predictions made by the model. In conjunction with this, the temporal and spatial variation of sine function fit and peak hour is investigated.

Singer et al. (2004) have presented an analysis noting an annual variation of the diurnal shift, whilst Singer et al. (2005) observe an inverse proportionality between latitude and intensity. The data available for my own study covers a larger range of latitudes, perhaps supporting either of these studies. There are over 3.8 million available hourly counts, providing a large sample from which analysis of temporal variation can be made.

2 Modelling the diurnal variation mechanism

For a detailed overview of the 'standard' explanation for the mechanism behind diurnal variation, see Hines (1956). Despite being detailed, Hines (1956) is not a mathematical formulation of the explanation. I put forward a model with the aim of a more complete and mathematically rigorous description.

First, I assume that the number of meteors detected is proportional to the mean incident velocity of meteors to Earth. This is reasonable: the actual velocities are of course random. However, an overall larger mean incident velocity of a collection of meteors means that proportionally more will reach Earth, of those that are in a direction that could cause a collision with Earth's atmosphere. Of a group of meteors with random velocities (both random magnitude and direction), very few will be on a course tangential to Earth's atmosphere. However, this does not change as Earth rotates, so it is a negligible variable. I consider only those that are tangential with the atmosphere, and so only those that could cause a detection. We have, at a very basic level:

$$N \propto v_{\text{incident}} \tag{1}$$

The incident velocity is dependent on factors such as the Earth's rotational velocity, orbital velocity and the velocity of the sporadic meteors themselves. v_{meteor} is difficult to consider, since it (theoretically) has a random direction. We know that $v_{\text{orbit}} \approx 30\,000\,\text{ms}^{-1}$ and $v_{\text{rotation}} \approx 450\,\text{ms}^{-1}$.

Assuming that the path described by Earth's orbit around the Sun is a straight line through Earth when 'up close', let θ be the angle between a radius from Earth's centre to the observer's location, and the orbital path (Figure 1).

The set of meteors that can be detected appear, looking from above Earth's pole, to form a triangle. The average velocity of these meteors will be along the height of this triangle, perpendicular to the surface of Earth (v_{meteor}). This is clear simply from how meteor showers appear: all meteors appear to originate from the radiant. Since this perpendicular velocity v_{meteor} remains perpendicular despite Earth's rotation, the rotational velocity of Earth can be disregarded. Thus, the

[1]Exeter Mathematics School, Exeter, Devon, EX4 3PU, United Kingdom
[2]Norman Lockyer Observatory, Sidmouth, Devon, EX10 0NY, United Kingdom
[3]Email: cpowell@cwp.io

IMO bibcode WGN-452-powell-diurnalshift
NASA-ADS bibcode 2017JIMO...45...32P

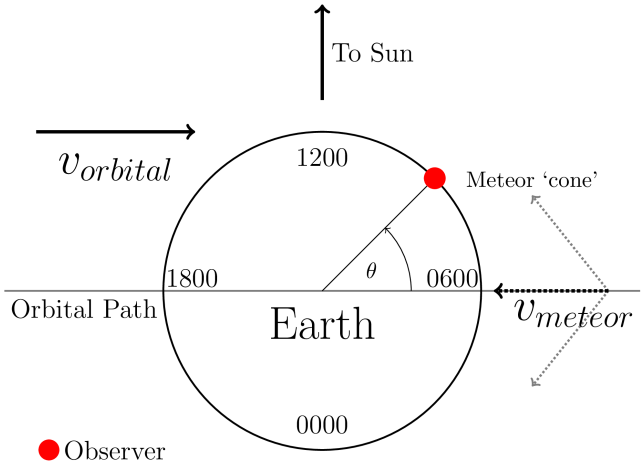

Figure 1 – Model diagram: Earth in orbit, showing an observer (red dot), the perceived meteor 'cone', and the incident meteor velocity v_{meteor}.

remaining velocity to consider is Earth's orbital velocity:

$$v_{\text{incident}} \approx v_{\text{orbit}} \cos\theta + v_{\text{meteor}} \tag{2}$$

Clearly, this is at a maximum when $\theta = 0°$. For an observer at a longitude of 0°, this is 6:00. Since this is where the angle is defined from, it is clear that for any observer the peak hour will be 6:00[a] local time (assuming local time is based on longitude, not timezones). It should be noted that the peak hour can vary around this time, based on conditions for observing. Particularly important are changes in electron concentration in the ionosphere as the Sun rises, which increases reflection of radio signals, allowing for better reception of signals reflected by ionised meteor trails (Rana & Yadav, 2014). This could shift the peak hour. This effect may also contribute to a change in diurnal shift intensity with latitude, since the increased atmospheric ionisation caused by the Sun is dependent on latitude (Dabas, 2000).

3 Methodology

I use previous results to examine spatial and temporal variation of diurnal shift, including a measure of goodness-of-fit between a sine function and the diurnal shift curve.

3.1 Data source

The data used is a database of hourly detection counts from almost 350 observers across the globe, provided by the Radio Meteor Observation Bulletin (RMOB), accessible at `www.rmob.org`.

3.2 Sine function fit

The diurnal shift curve is generated by taking the mean of all data for a given hour after midnight for each observer. Time, for all observers, is recorded in UTC.

[a]All times given in 24-hour format

Table 1 – Sample sizes for location categories

Category	N° observers
Europe	220
Asia & Australia	12
North America	37

Using this curve I will compare the intensity of diurnal shift for three different location categories: Europe, Asia & Australia, and North America. The sample sizes for each category are shown in Table 1. Observers are sorted into these categories based on metadata provided with the RMOB data. In conjunction with this, I fit a sine curve, in order to test the model, indicating how well diurnal shift is described by a sinusoidal function.

3.3 Spatial analysis

QGIS (QGIS Development Team, 2009) is used to generate a map, with a dot representing each observer with a known location. These dots will be coloured based on the peak hour of diurnal shift, indicating how this changes with location. Further to this, I will analyse the variation of the peak hour of diurnal shift, as well as the error in fit for a sine function of the form $A\sin\left(\frac{2\pi}{24}t + \phi\right) + \mu$, indicating how well a sine curve fits the diurnal shift. This is calculated using the reduced covariance matrix X and the reduced chi-squared χ^2, where

$$\chi^2 = \frac{r^T I r}{N - 3} \tag{3}$$

N is the number of data points, r is the matrix of residuals and I is the identity matrix. The numerator is the minimum value of the weighted objective function (the optimal parameters). Then the variance-covariance matrix of the parameters M^β is;

$$M^\beta = \chi^2 \left(X^T X\right)^{-1} \tag{4}$$

The parameter standard deviations is $\sigma_i = \sqrt{M^\beta_{ii}}$, and the sum of these three is taken. This analysis will be over two independent variables: latitude and longitude.

3.4 Temporal analysis

Finally I analyse how the peak hour and sinusoidal function fit vary over time, from 2000 to 2016. This will use the same calculated variables as the spatial analysis. These analyses will be completed using a Python program.

4 Results & Discussion

4.1 Sine function fit

Figure 2 shows the results for sine function fit. The optimal sine function and cubic are shown in red and green respectively. The sum of parameter standard deviations of the optimal sinusoidal function is 0.814, which indicates a good fit. This suggests that the sine function fits well. As a reference, a cubic is fitted. This shows

how well a sine curve fits in comparison. This suggests that the cause of diurnal shift is based on a sine function of Earth's rotation (i.e. the hour of the day), which supports the presented model.

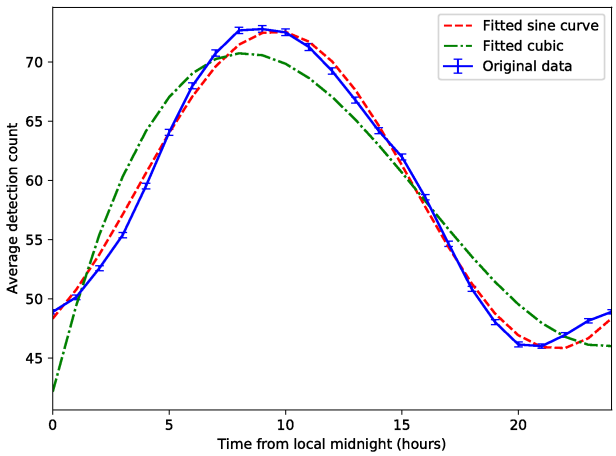

Figure 2 – Diurnal shift across all authors & sine function fit.

Figure 3 shows the same plot as Figure 2 for comparison, as well as diurnal shift curves for each respective location. "All" refers to the set of data from all observers. Surprisingly, each location category shows a clear sine curve. The peak of these sine curves appears to be correlated well with latitude. The average longitudes are, for Europe, Asia & Australia, and North America respectively: $\sim 15°$, $\sim 150°$ & $\sim -100°$. This supports the idea that the sine function can be used to describe the diurnal shift, since larger longitudes produce a greater hour of diurnal shift. The average latitudes are (respectively): $\sim 45°$, $\sim 35°$ & $\sim 15°$. The North American category has the largest intensity, followed by the European category and then Asia & Australia, though this is not the order of latitudes (seen in Figure 4). This appears to disagree with Singer et al. (2005), where it was suggested that the intensity (amplitude) of diurnal shift is dependent on latitude. It is difficult to comment on why the intensity of one category is different to another without knowledge of the exact detection setup, antenna type and observing conditions for a given observer.

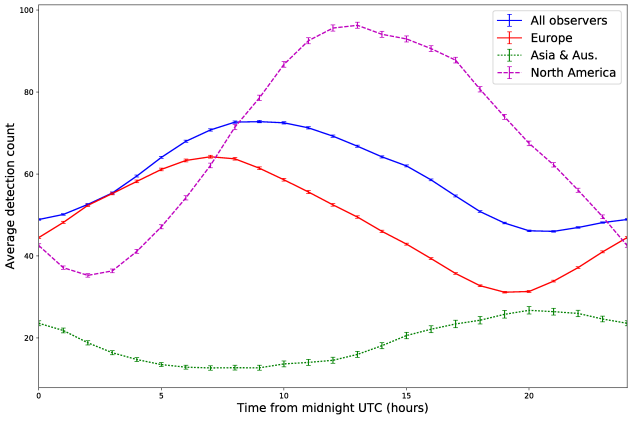

Figure 3 – Diurnal shifts for each individual location (overall shift of all observers included for reference).

Table 2 – Diurnal shift parameter results for location categories. Column 5 contains the sum of parameter standard deviations.

Category	A	ϕ	μ	$\Sigma\sigma$
All	13.4	−0.941	59.2	0.454
Europe	15.4	−0.302	48.4	0.498
Asia & Aus.	−7.19	−0.585	19.0	0.352
N. America	29.5	−2.05	68.1	1.16

The sum of parameter standard deviations for each location category are shown below. The positive numbers all indicate a positive correlation, as expected from the figures. Again, "all" refers to the diurnal shift curve when including data from all observers.

4.2 Spatial variation

Figure 4 contains a map showing the location of each observer in the data set. The dot for each circle is coloured (as in the legend) based on the peak hour of the diurnal shift. This gives a more visual demonstration of what is shown in Figures 3 and 7: the colours are clearly grouped based on location. Observers in Europe have diurnal shift peaks mostly around 6:00, North American observers have peaks around 15:00 and in Asia & Australia around 20:00. This supports implications from the previously stated figures. There are clearly anomalous results for some observers (note the blue dots in Europe), though there is often anomalous data, so this is not unexpected.

Latitude

There appears to be little correlation between latitude and the peak hour. Although, overall, the hour appears to decrease as the latitude varies from $-40°$ to $60°$, the error bars, indicating standard error, are substantial. The implication of this is there is little agreement within each category, suggesting no correlation at all. However, this is expected. There is no logical reason why the peak hour would be influenced by the latitude. Diurnal shift is modelled as being caused by Earth's rotation changing the average incident velocity of meteors. This does not change with latitude, hence no correlation is seen.

In Figure 6, little correlation is seen again. The standard deviations vary widely. There is no clear trend, suggesting that the latitude of an observer has no effect on how well collected data fits a sine function. Consequently, it would appear location does not influence diurnal shift.

Singer et al. (2005) analyse a variation of diurnal shift amplitude with latitude, over a relatively small range of latitudes. I find no correlation to support this finding, though the distribution of observer latitudes for my study is not uniform, making a definite conclusion difficult.

Longitude

Figure 7 shows agreement with Figures 3 and 4. The peak hour is lowest for a longitude of $0°$ and increases

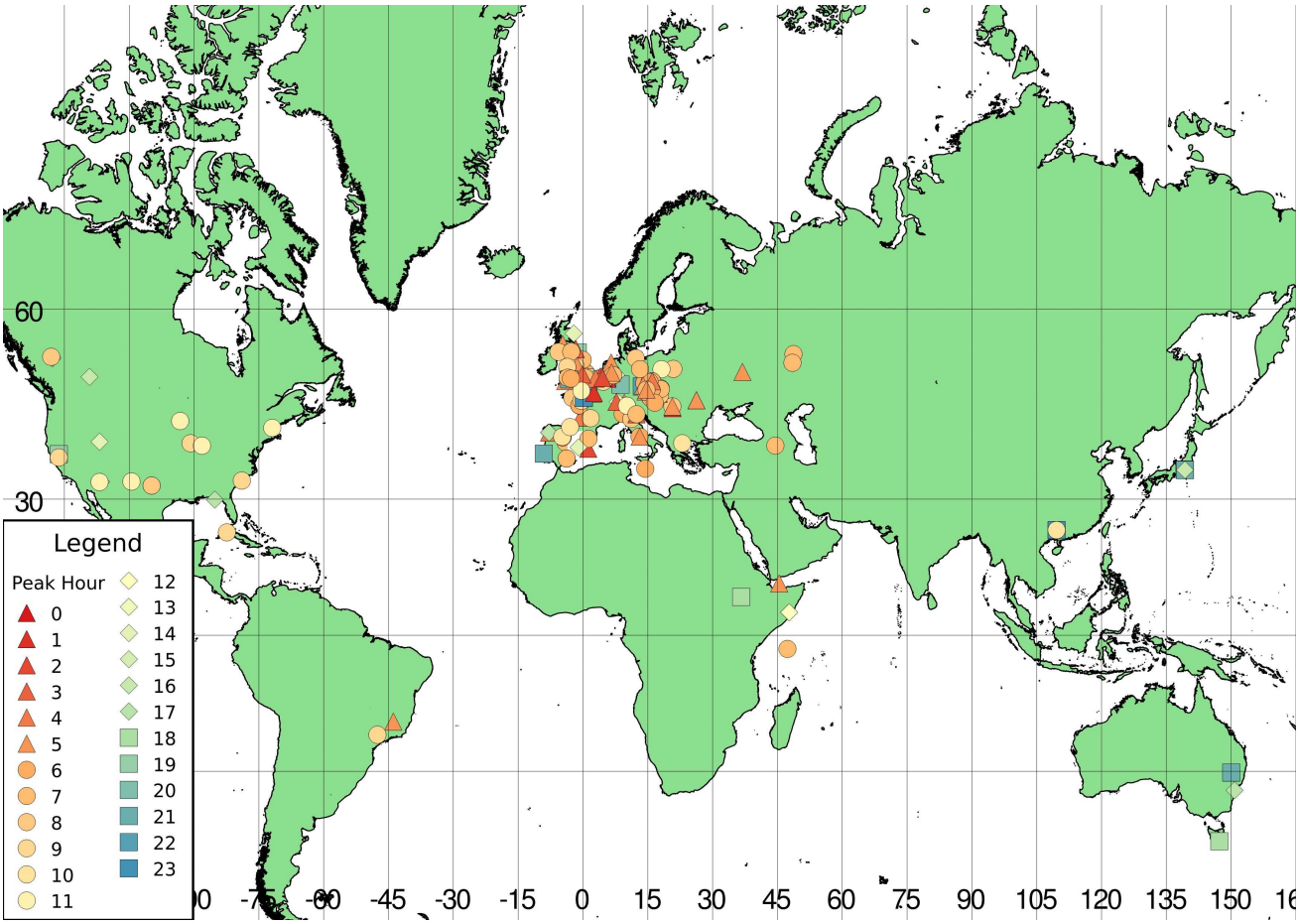

Figure 4 – Peak hour of diurnal shift for each observer.

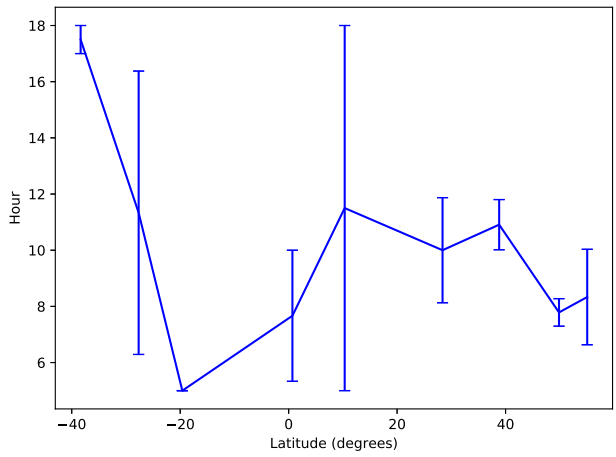

Figure 5 – Peak hour of diurnal shift against latitude.

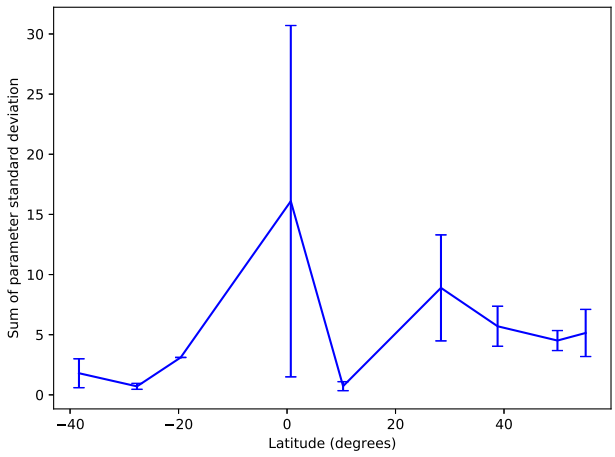

Figure 6 – Optimal sine function fit against latitude.

either side of this, as seen in the stated figures. The errors for some categories are reasonably large, though still fall in a range that fits the trend. There is, of course, minor variation though the trend is clear from the data: latitude and peak hour of diurnal shift are related.

In order to investigate this apparent trend further, I have corrected the peak hour of each location category such that $H_{\text{corrected}} = H_{\text{calculated}} + \frac{\phi}{15}$, provided the longitude ϕ is in degrees. This means that the hour will be the local time (not using timezones, only the time based on longitude). This is shown in Figure 8. Error bars, in this case, are such that 75% of the data for a given location category falls within the bars. The values appear to fluctuate around a peak hour of 6:00 (shown in green), supporting the model I have proposed. However, there is a large degree of variation.

In Figure 9 a histogram of the peak hour is shown. It is clear from this figure that the model is supported. Clearly most of the observers have a peak hour around

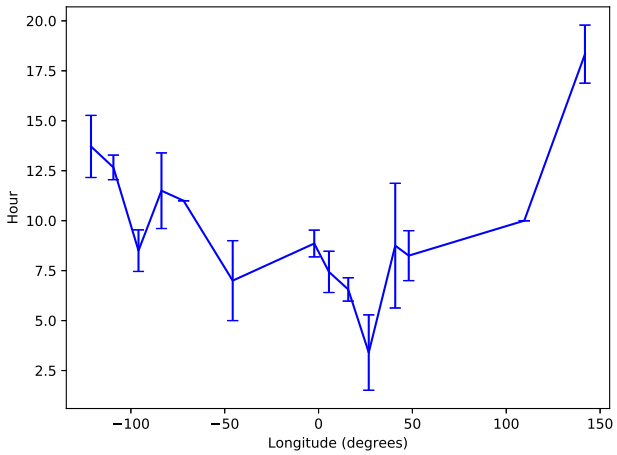

Figure 7 – Peak hour of diurnal shift against longitude.

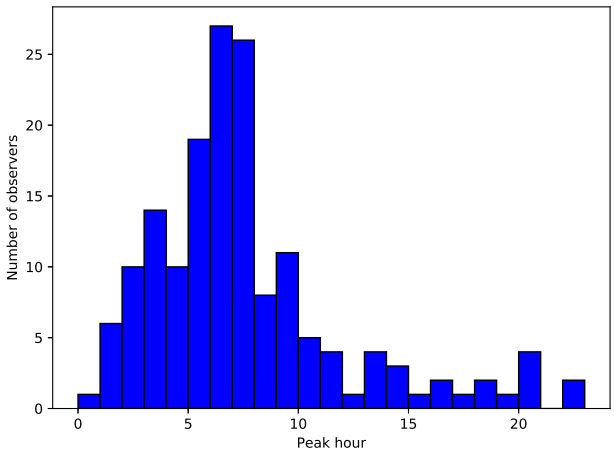

Figure 9 – Histogram of peak hours.

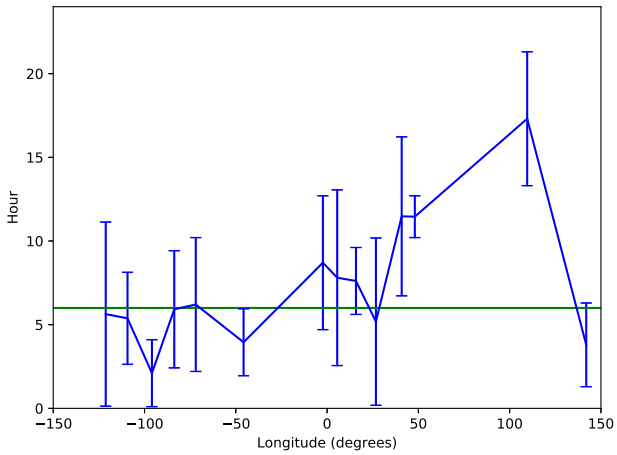

Figure 8 – Corrected peak hour of diurnal shift against longitude.

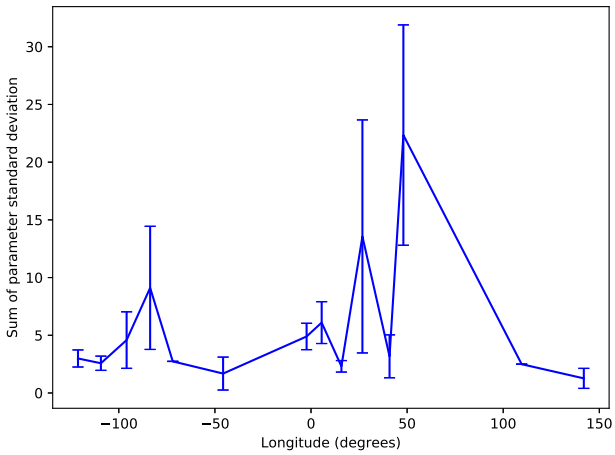

Figure 10 – Optimal sine function fit against longitude.

6, with some having a peak hour of 7. This is reasonable; as noted in section 2, the peak hour can vary slightly, resulting in some distribution either side of 6:00, so this is expected.

Most meteor detection setups are simply receiving stations. Typically a station, often a considerable distance away, emits a signal that reflects off the meteor's ionised trail and is received by the observer. This means that there is a difference between the longitude of the observer and the longitude of where the detection takes place. This is likely to have caused the observed distribution.

The sum of parameter standard deviations, indicating fit, varies a small amount with longitude for most categories. However, some have much greater variation, indicating less consistency in the data. There does not appear to be a clear trend. However, the poorest fits have large errors indicating that this is not a poor fit throughout observers in said categories. Consequently it would seem that the fit varies moderately across the globe.

4.3 Temporal variation

Figure 11 shows the same result as previously noted, namely a general diurnal behaviour. The peak hour for each location category varies around the hours expected, given that peak hour is correlated with longitude. There is a large amount of variation for the Asia & Australia category, so it is hard to make an analysis from this. It is clear that in more recent years, there is less variation. However, in general, no categories appear to increase or decrease over time, suggesting that the diurnal behaviour is constant, and not subject to a large degree of seasonal or annual change.

Generally, the fit, shown in Figure 12 is reasonably good. The fit may be considered a measure of the consistency of data obtained by each station. Thus the data indicates that there is less consistent data obtained between 2005 and 2011, since the fits are much poorer. This indicates either a weaker diurnal shift (an unlikely occurence) or a greater background detection rate. For periods outside this range, there is a low amount of variation. All categories have a similar fit and absent trend over time.

A question that may require a more detailed model of the mechanism behind diurnal shift is whether the phenomenon changes on a yearly time scale. Seasonal variation of diurnal shift may indicate an influence from sources such as the Sun, or the orientation of the Earth relative to its orbit. I do not make such an analysis, leaving scope for this in the future.

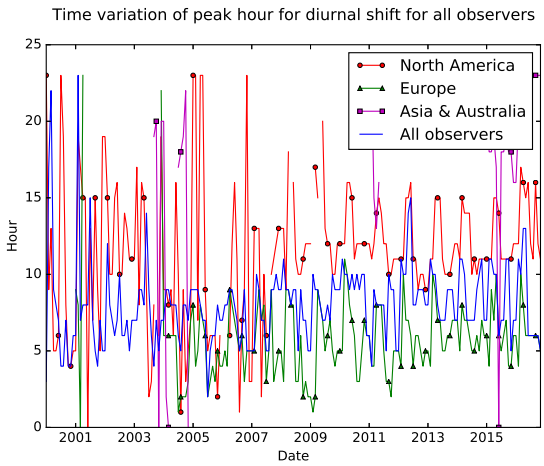

Figure 11 – Peak hour of diurnal shift change over time.

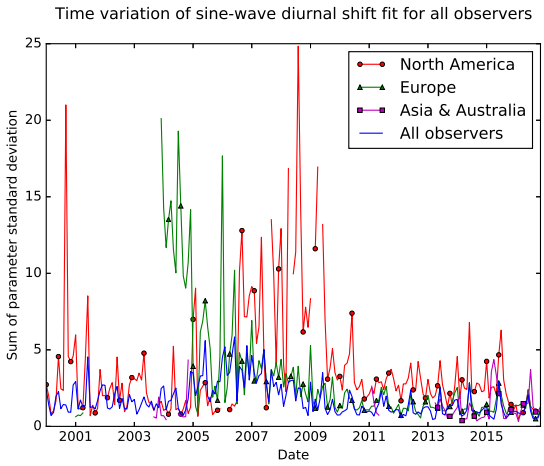

Figure 12 – Optimal sine function fit change over time.

5 Conclusion

1. There is a clear correlation between longitude and peak hour of diurnal shift, as suggested by the proposed model. This is apparent from several results, including a histogram of peak hours.

2. The good agreement indicates that the proposed model is a valid explanation of the mechanism and is supported by the data. Thus it can be concluded that the influence of orbital velocity on incident meteor velocity is the primary mechanism behind diurnal shift.

3. There is little correlation between location and a sine function fit, suggesting that the intensity of diurnal shift (in the sense of relative intensity compared to background detection rates) is roughly uniform across the globe.

4. There is no clear link to be made between the intensity of diurnal variation and latitude.

5. There are differences in amplitude between different location categories, however I find no explanation for this.

6. During the period of increased detection rates, the relative intensity of diurnal variation decreases.

6 Acknowledgements

Permission for use of data is kindly provided by the RMOB organisation[b], compiled by Chris Stayeart and hosted by Pierre Terrier. This work has in part been supported by the Norman Lockyer Observatory[c] and Exeter Mathematics School[d].

References

Dabas R. S. (2000). "Ionosphere and its influence on radio communications". *Resonance*, **5:7**, 28–43.

Hines C. O. (1956). "Diurnal variations in forward-scacattered meteor signals". *Journal of Atmospheric and Terrestrial Physics*, **9:4**, 229–232.

Kero J., Szasz C., Nakamura T., Meisel D. D., Ueda M., Fujiwara Y., Terasawa T., Nishimura K., and Watanabe J. (2012). "The 2009–2010 MU radar head echo observation programme for sporadic and shower meteors: radiant densities and diurnal rates". *MNRAS*, **425**, 135–146.

Okamoto S. and Maegawa K. (2008). "Annual and diurnal variation of meteor rates by the forward-scatter radio observation". *Earth, Moon, and Planets*, **103**, 65–68.

QGIS Development Team (2009). *QGIS Geographic Information System*. Open Source Geospatial Foundation.

Rana G. and Yadav M. K. (2014). "The ionosphere and radio propagation". *IJECET*, **5:11**, 9–16.

Singer W., von Zahn U., Batista P. P., Fuller B., and Latteck R. (2005). "Diurnal and annual variations of meteor rates at latitudes betwen 69°N and 35°S". *17th ESA Symposium on European Rocket and Balloon Programmes and Related Research*, pages 151–156.

Singer W., von Zahn U., and Weiß J. (2004). "Diurnal and annual variations of meteor rates at the arctic circle". *Atmos. Chem. Phys.*, **4**, 1355–1363.

Handling Editor: Jürgen Rendtel
This paper has been typeset from a LaTeX file prepared by the author.

[b] http://www.rmob.org
[c] http://www.normanlockyer.com
[d] http://www.exetermathematicsschool.ac.uk

Short communication

June theta Serpentids (IAU#683, JTS) confirmed

Peter Jenniskens[1]

The June theta Serpentids (IAU#683, JTS) shower is confirmed from CAMS, SonotaCo, Edmond, and CMN video-detected meteor orbits.

Received 2017 March 25

1 Introduction

CAMS earlier yielded the detection of a new shower, the June theta Serpentids (IAU#683, JTS), with 11 video-detected meteors radiating from geocentric RA = 284.°2, Dec = +1.°5 with speed V_g = 36.9 km/s around solar longitude 91° (Jenniskens et al., 2016). The shower is caused by an unidentified prograde-moving long-period comet. In order to confirm this shower from the ongoing SonotaCo[a], Edmond[b], and CMN[c] video-detected meteor surveys, a wide net was thrown around the position of the shower in the combined database by selecting all meteors with RA = 260–300°, Dec = −10° to +10°, and V_g = 30–50 km/s during the solar longitude interval 60–100°. On closer inspection, no shower members were detected before solar longitude 81.°0 and after 94.°0. The shower stands out well in the remaining data (Figure 1).

Crosses mark the extracted shower members. In addition to the initial 11 reported members (2010–2012 data), CAMS added another 11 shower members in 2013–2015. The shower is confirmed from a detection of 6 shower members in the SonotaCo database (2007–2015), while Edmond and CMN each added 1.

The histogram of Figure 1 shows the shower activity. Period of activity is 81.°6–93.°4 solar longitude, with a median value of 86.°9 (all data). The updated median orbital elements are listed in Table 1.

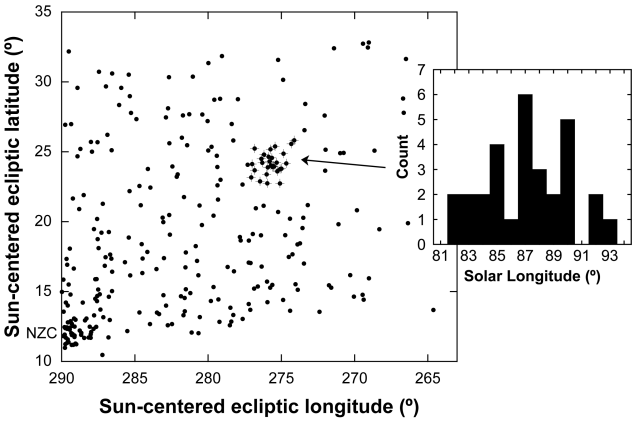

Figure 1 – Detection of June theta Serpentids in the 81–94° solar longitude interval from combined video data 2007–2015.

References

Jenniskens P., Nénon Q., Gural P. S., Albers J., Haberman B., Johnson J., Morales R., Grigsby B. J., Samuels D., and Johannink C. (2016). "CAMS newly detected meteor showers and the sporadic background". *Icarus*, **266**, 384–409.

Handling Editor: Javor Kac

[1]SETI Institute, Mountain View, California. USA.
Email: petrus.m.jenniskens@nasa.gov

IMO bibcode WGN-452-jenniskens-jts
NASA-ADS bibcode 2017JIMO...45...38J

[a]http://sonotaco.jp/doc/SNM/
[b]http://www.daa.fmph.uniba.sk/edmond
[c]http://cmn.rgn.hr/

Table 1 – Median geocentric radiant, speed, and orbital elements.

$\lambda_\odot$ (°)	RA (°)	Dec (°)	V_g (km/s)	a (AU)	q (AU)	e	ω (°)	Node (°)	i (°)	N	Source
87.7	281.0	+1.1	36.9	22.99	0.386	0.983	284.0	87.7	35.9	22	this work, CAMS
85.6	279.5	+1.1	36.4	10.91	0.385	0.964	285.0	85.6	36.2	6	this work, SonotaCo
(87.7)	281.2	+1.2	36.9	16.96	0.389	0.984	283.5	89.3	35.9	11	Jenniskens et al. 2016

Preliminary results

Results of the IMO Video Meteor Network — October 2016

Sirko Molau[1], *Stefano Crivello*[2], *Rui Goncalves*[3], *Carlos Saraiva*[4], *Enrico Stomeo*[5], *and Javor Kac*[6]

More than 47 000 meteors were recorded in almost 9 200 hours of observing time in 2016 October by 81 cameras of the IMO Video Meteor Network. The flux density profile of the Orionids is presented, showing enhanced flux density above the long-term average between October 18 and 20. The flux density profiles are also shown for the Northern and Southern Taurids, October Camelopardalids, and October Ursae Majorids.

Received 2016 December 29

1 Introduction

Similar to previous years, the fine weather took a break in October. After fireworks of clear nights with the climax in Indian summer, we switched to autumn melancholy with cloudy and rainy weather. Our statistics shows many gaps and the number of observing nights per camera reduced noticeable. Whereas in September almost 90% of the cameras observed in twenty or more nights, it was only 60% in October. In one third of September nights we counted at least 70 active cameras. In October that happened in one tenth of the nights only, even though there were two cameras more active than in September. With overall 47 000 meteors from 9200 hours of effective observing time (Table 1 and Figure 1), the output of the IMO Video Network was below the average of the previous five years.

Stefano Crivello observed with his camera STG38 between June 26 and October 11 without a single break, which add up to 108 observing nights in a row. That is probably unique in the history of the IMO Network.

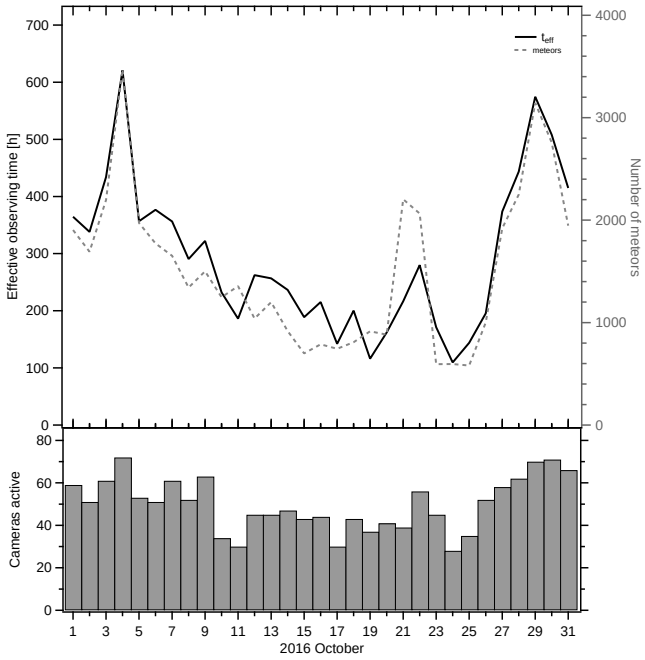

Figure 1 – Monthly summary for the effective observing time (solid black line), number of meteors (dashed gray line) and number of cameras active (bars) in 2016 October.

2 Orionids

As for meteor activity, October is a wealthy month with the Orionids and a number of minor showers, not to forget that also the sporadic rate reaches peak values. The most important shower, however, was tainted twice in 2016. The lunar phase was quite unfavourable, since the waning moon was located close to the Orionid radiant at the time of maximum, and also the weather was particularly poor until the middle of the last third of the month. The overall profile (Figure 2, red) shows clearly enhanced flux density between October 18 and 20 (solar longitude 206–208°) which exceeds the long-term average (Figure 2, green) by up to a factor of two, whereas the activity profile matches nicely with the long-term average in the time before and thereafter. An independent confirmation would be desirable, but is not possible in the absence of visual data.

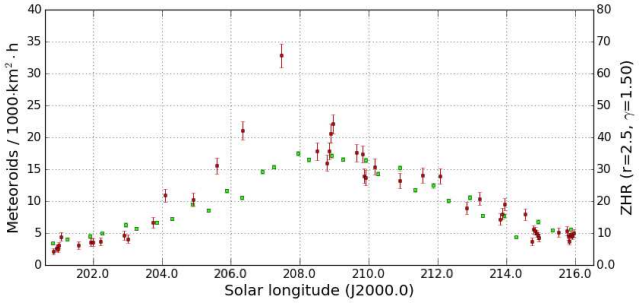

Figure 2 – Comparison of the flux density of the 2016 Orionids (red) with the average of the years 2011–2015 (green), derived from video data of the IMO Video Meteor Network.

[1]Abenstalstr. 13b, 84072 Seysdorf, Germany.
Email: sirko@molau.de
[2]Via Bobbio 9a/18, 16137 Genova, Italy.
Email: stefano.crivello@libero.it
[3]Urbanizacao da Boavista, Lote 46, Linhaceira, 2305-114 Asseiceira, Tomar, Portugal. Email: rui.goncalves@ipt.pt
[4]Rua Aquilino Ribeiro, 23 - 1 Dto. 2790028 Carnaxide, Portugal. Email: carlos.saraiva@netcabo.pt
[5]via Umbria 21/d, 30037 Scorze (VE), Italy.
Email: stom@iol.it
[6]Na Ajdov hrib 24, 2310 Slovenska Bistrica, Slovenia.
Email: javor.kac@orion-drustvo.si

IMO bibcode WGN-452-molau-vidoct
NASA-ADS bibcode 2017JIMO...45...39M

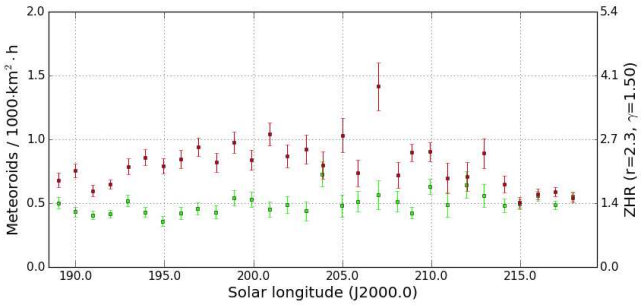

Figure 3 – Flux density profile of the Northern (green) and Southern Taurids (red) in October 2016, derived from video data of the IMO Video Meteor Network.

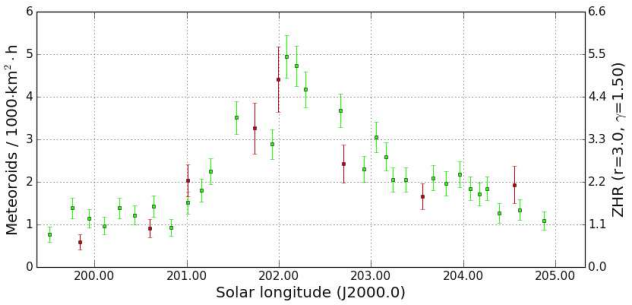

Figure 5 – Comparison of the flux density of the October Ursae Majorids 2016 (red) with the average of the years 2011–2015 (green), derived from video data of the IMO Video Meteor Network.

3 Taurids

If the result is compared with the Taurids, we get an inconsistent picture: Whereas Northern Taurid activity was nearly constant in all of October, we see enhanced Southern Taurid rates on October 20 as well (Figure 3). Hence, it cannot be ruled out, that both outliers result at least partly from data with stronger scatter because of poor circumstances.

4 October Camelopardalids

Looking at the October Camelopardalids of early October it is surprising that "outbursts" are predicted and observed. As we showed already in 2009, this is an annual shower which can typically be observed only every few years at a particular site because of its short duration. The peak predicted by Esko Lyytinen (Rendtel, 2015) for the afternoon hours of October 5 (solar longitude 192.°56) matches to the maximum observed in previous years. Hence, it is not really a surprise that both Finnish video systems and Japanese forward scatter systems detected "enhanced" rates. The IMO Network cameras were not active by that time, but the activity profiles since 2011 (Figure 4, top) show that the October Camelopardalid activity was observed at exactly the same time in other years. At the bottom of Figure 4 we present the averaged activity profile of the past six years. Peak flux density occurs at solar longitude 192.°58, which matches perfectly to the prediction.

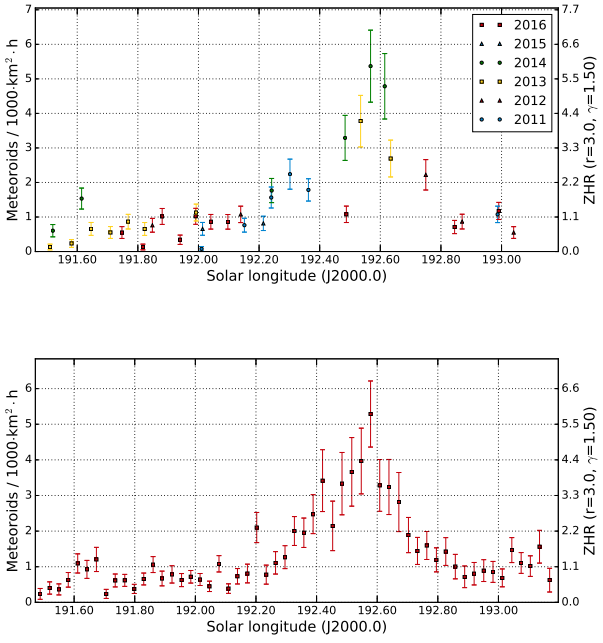

Figure 4 – Activity profile of the October Camelopardalids. The individual values of the years 2011–2016 are shown at the top, the average profile at the bottom.

5 Other minor showers of October

The other meteor showers of October provided no surprise either. The Draconids were virtually non-existent, the Leonis Minorids and ε-Geminids showed a low activity level without a clear peak, and the activity profile of the October Ursae Majorids fits well to the observations of previous years (Figure 5).

References

Rendtel J. (2015). "2016 Meteor Shower Calendar". International Meteor Organization. IMO INFO(2-15).

Handling Editor: Javor Kac

Code	Name	Location	Camera	FOV [°²]	Stellar LM [mag]	Eff.CA [km²]	Nights	Time [h]	Meteors
ARLRA	Arlt	Ludwigsfelde/DE	Ludwig2 (0.8/8)	1475	6.2	3779	21	95.4	788
BANPE	Bánfalvi	Zalaegerszeg/HU	Huvcse01 (0.95/5)	2423	3.4	361	11	44.0	65
BERER	Berkó	Ludányhalászi/HU	Hulud1 (0.8/3.8)	5542	4.8	3847	6	46.1	383
BOMMA	Bombardini	Faenza/IT	Mario (1.2/4.0)	5794	3.3	739	22	140.6	939
BREMA	Breukers	Hengelo/NL	Mbb3 (0.75/6)	2399	4.2	699	26	132.2	475
BRIBE	Klemt	Herne/DE	Hermine (0.8/6)	2374	4.2	678	23	116.1	485
		Bergisch Gladbach/DE	Klemoi (0.8/6)	2286	4.6	1080	23	124.9	541
CARMA	Carli	Monte Baldo/IT	Bmh2 (1.5/4.5)*	4243	3.0	371	23	150.9	540
CASFL	Castellani	Monte Baldo/IT	Bmh1 (0.8/6)	2350	5.0	1611	24	174.7	858
CRIST	Crivello	Valbrevenna/IT	Bilbo (0.8/3.8)	5458	4.2	1772	26	161.3	924
			C3P8 (0.8/3.8)	5455	4.2	1586	20	142.8	692
			Stg38 (0.8/3.8)	5614	4.4	2007	26	172.6	1424
DONJE	Donani	Faenza/IT	Jenni (1.2/4)	5886	3.9	1222	23	148.6	1049
ELTMA	Eltri	Venezia/IT	Met38 (0.8/3.8)	5631	4.3	2151	19	133.1	711
FORKE	Förster	Carlsfeld/DE	Akm3 (0.75/6)	2375	5.1	2154	8	40.0	178
GONRU	Goncalves	Foz do Arelho/PT	Farelho1 (1.0/2.6)	6328	2.8	469	24	118.8	185
		Tomar/PT	Templar1 (0.8/6)	2179	5.3	1842	23	194.2	895
			Templar2 (0.8/6)	2080	5.0	1508	23	193.8	683
			Templar3 (0.8/8)	1438	4.3	571	24	165.3	265
			Templar4 (0.8/3.8)	4475	3.0	442	23	187.0	608
			Templar5 (0.75/6)	2312	5.0	2259	26	167.3	654
GOVMI	Govedič	Središče ob Dravi/SI	Orion2 (0.8/8)	1447	5.5	1841	21	141.0	585
			Orion4 (0.95/5)	2662	4.3	1043	19	124.4	332
HERCA	Hergenrother	Tucson/US	Salsa3 (0.8/3.8)	2336	4.1	544	31	325.7	1255
HINWO	Hinz	Schwarzenberg/DE	Hinwo1 (0.75/6)	2291	5.1	1819	15	41.6	175
IGAAN	Igaz	Hódmezővásárhely/HU	Huhod (0.8/3.8)	5502	3.4	764	20	37.4	223
		Budapest/HU	Hupol (1.2/4)	3790	3.3	475	5	22.6	21
JONKA	Jonas	Budapest/HU	Husor (0.95/4)	2286	3.9	445	14	93.1	254
			Husor2 (0.95/3.5)	2465	3.9	715	17	101.9	315
KACJA	Kac	Ljubljana/SI	Orion1 (0.8/8)	1399	3.8	268	15	84.4	241
		Kamnik/SI	Cvetka (0.8/3.8)*	4914	4.3	1842	13	76.9	355
			Rezika (0.8/6)	2270	4.4	840	13	99.6	784
			Stefka (0.8/3.8)	5471	2.8	379	13	72.6	224
		Kostanjevec/SI	Metka (0.8/12)*	715	6.4	640	3	21.0	72
KOSDE	Koschny	Izana Obs./ES	Icc7 (0.85/25)*	714	5.9	1464	25	168.0	1666
			Lic1 (2.8/50)*	2255	6.2	5670	27	194.7	2560
		La Palma/ES	Icc9 (0.85/25)*	683	6.7	2951	28	199.8	2465
			Lic2 (3.2/50)*	2199	6.5	7512	27	221.0	2922
LOJTO	Łojek	Grabniak/PL	Pav57 (1.0/5)	1631	3.5	269	4	22.6	98
LOPAL	Lopes	Lisbon/PT	Naso1 (0.75/6)	2377	3.8	506	19	106.8	261

Table 1 – Observers contributing to 2016 October data of the IMO Video Meteor Network. Eff.CA designates the effective collection area; the overall number of nights is the number of nights with at least one camera operating, the overall observing time and number of meteors are sums over all cameras.

Table 1 – Observers contributing to 2016 October data of the IMO Video Meteor Network – continued from previous page.

Code	Name	Location	Camera	FOV [°²]	Stellar LM [mag]	Eff.CA [km²]	Nights	Time [h]	Meteors
MACMA	Maciejewski	Chełm/PL	Pav35 (0.8/3.8)	5495	4.0	1584	15	64.1	303
			Pav36 (0.8/3.8)*	5668	4.0	1573	18	82.6	408
			Pav43 (0.75/4.5)*	3132	3.1	319	15	72.8	232
			Pav60 (0.75/4.5)	2250	3.1	281	20	91.3	475
MARGR	Maravelias	Lofoupoli-Crete/GR	Loomecon (0.8/12)	738	6.3	2698	12	94.7	192
MARRU	Marques	Lisbon/PT	Cab1 (0.75/6)	2362	4.8	1517	29	181.7	674
			Ran1 (1.4/4.5)	4405	4.0	1241	26	161.4	572
MASMI	Maslov	Novosibirsk/RU	Nowatec (0.8/3.8)	5574	3.6	773	3	26.6	133
MOLSI	Molau	Seysdorf/DE	Avis2 (1.4/50)*	1230	6.9	6152	26	132.4	1402
			Escimo2 (0.85/25)	155	8.1	3415	24	129.7	451
			Mincam1 (0.8/8)	1477	4.9	1084	22	123.6	819
		Ketzür/DE	Remo1 (0.8/8)	1467	6.5	5491	21	97.3	882
			Remo2 (0.8/8)	1478	6.4	4778	21	100.2	701
			Remo3 (0.8/8)	1420	5.6	1967	20	89.2	332
			Remo4 (0.8/8)	1478	6.5	5358	20	100.1	728
MORJO	Morvai	Fülöpszállás/HU	Huful (1.4/5)	2522	3.5	532	22	128.1	314
MOSFA	Moschini	Rovereto/IT	Rover (1.4/4.5)	3896	4.2	1292	22	28.0	167
OTTMI	Otte	Pearl City/US	Orie1 (1.4/5.7)	3837	3.8	460	22	103.1	341
PERZS	Perkó	Becsehely/HU	Hubec (0.8/3.8)*	5498	2.9	460	3	8.1	73
ROTEC	Rothenberg	Berlin/DE	Armefa (0.8/6)	2366	4.5	911	11	60.4	173
SARAN	Saraiva	Carnaxide/PT	Ro1 (0.75/6)	2362	3.7	381	24	143.0	346
			Ro2 (0.75/6)	2381	3.8	459	27	138.0	509
			Ro3 (0.8/12)	710	5.2	619	28	182.4	809
			Sofia (0.8/12)	738	5.3	907	27	154.6	410
SCALE	Scarpa	Alberoni/IT	Leo (1.2/4.5)*	4152	4.5	2052	22	145.4	303
SCHHA	Schremmer	Niederkrüchten/DE	Doraemon (0.8/3.8)	4900	3.0	409	22	138.4	524
SLAST	Slavec	Ljubljana/SI	Kayak1 (1.8/28)	563	6.2	1294	14	86.4	320
			Kayak2 (0.8/12)	741	5.5	920	13	84.7	122
STOEN	Stomeo	Scorze/IT	Min38 (0.8/3.8)	5566	4.8	3270	23	139.5	1214
			Noa38 (0.8/3.8)	5609	4.2	1911	23	143.1	1023
			Sco38 (0.8/3.8)	5598	4.8	3306	22	143.6	1411
STRJO	Strunk	Herford/DE	Mincam2 (0.8/6)	2354	5.4	2751	23	98.6	581
			Mincam3 (0.8/6)	2338	5.5	3590	20	86.7	316
			Mincam4 (1.0/2.6)	9791	2.7	552	11	54.2	41
			Mincam5 (0.8/6)	2349	5.0	1896	20	85.0	345
			Mincam6 (0.8/6)	2395	5.1	2178	21	87.3	347
TEPIS	Tepliczky	Agostyán/HU	Huago (0.75/4.5)	2427	4.4	1036	19	104.1	335
			Humob (0.8/6)	2388	4.8	1607	17	100.2	418
TRIMI	Triglav	Velenje/SI	Sraka (0.8/6)*	2222	4.0	546	18	80.6	199
WEGWA	Wegrzyk	Nieznaszyn/PL	Pav78 (0.8/6)	2286	4.0	778	16	44.4	221
YRJIL	Yrjölä	Kuusankoski/FI	Finexcam (0.8/6)	2337	5.5	3574	10	64.2	261
* active field of view smaller than video frame						Overall	31	9 184.6	47 587

Results of the IMO Video Meteor Network — November 2016

Sirko Molau[1], *Stefano Crivello*[2], *Rui Goncalves*[3], *Carlos Saraiva*[4], *Enrico Stomeo*[5], *and Javor Kac*[6]

Almost 43 000 meteors were recorded in more than 7 700 hours of observing time in 2016 November by 79 cameras of the IMO Video Meteor Network. The flux density profile of the 2016 Leonids that is presented fits perfectly to the average flux density profile for the years 2011, 2012, 2014 and 2015. No activity enhancement could be noted. The average flux density profile of the α-Monocerotids from the years 2011–2016 is presented, showing very low activity throughout. Finally, the flux density profiles are presented for the Northern and Southern Taurids.

Received 2017 May 3

1 Introduction

Taking into consideration that November weather is typically wet and cold in central Europe, the second-to-last month of 2016 provided relative good observing conditions – better than in many earlier years. However, it could not compare with the record-breaking month of November 2015. An overall total of 79 cameras contributed to the IMO Network and more than half of these managed to observe on twenty or more nights. These included the new camera Ro4 of Carlos Saraiva, a Watec camera with a c-mount zoom lens that started regular observation in November. With over 9 700 hours, the effective observing total fell about 20% short of the 2015 result, and the number of meteors dropped by a larger 25% to 43 000 (Table 1 and Figure 1).

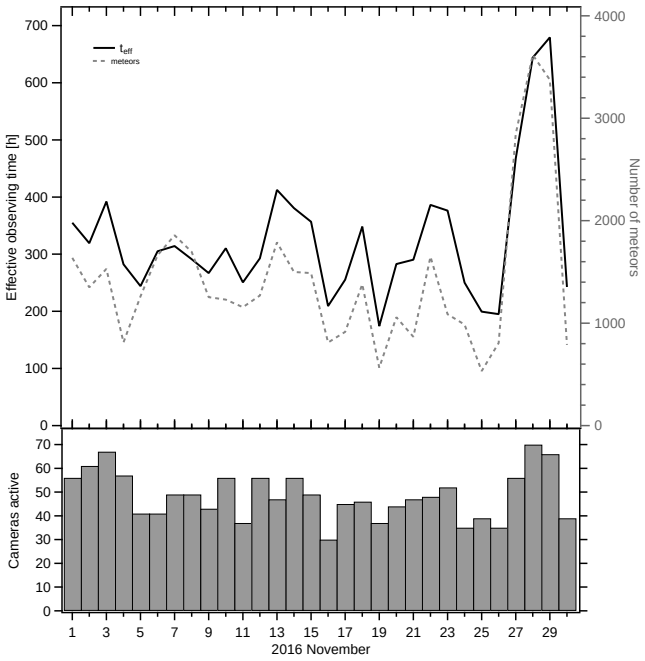

Figure 1 – Monthly summary for the effective observing time (solid black line), number of meteors (dashed gray line) and number of cameras active (bars) in 2016 November.

2 Leonids

With respect to meteor showers, November was not particularly thrilling. Far away from their famous outbursts at the onset of the millennium, the Leonids presented the usual activity profile with a slow increase starting at about 232° solar longitude (November 13), a peak activity of 7 meteoroids per 1 000 km^2 per hour between 236° and 238° solar longitude (November 17–19) and a steeper decrease until 240° solar longitude, corresponding to November 21 (Figure 2). As was the case for many major showers in 2016, the moon hampered the Leonid observations significantly. However, in the end our data confirmed the prediction that there would be no enhanced activity (Rendtel, 2015).

Figure 3 illustrates for the Leonids 2016 the impact of the new method to calculate the limiting magnitude loss from meteor motion. The new algorithm (which is not yet used) creates an activity profile with a similar shape, but the absolute ZHR and flux density values reduce about a factor of two compared to the previous method.

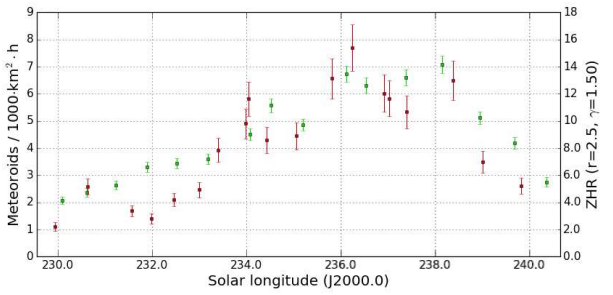

Figure 2 – Comparison of the flux density of the Leonids 2016 (red) with the average for the years 2011–2015 (green), derived from video data of the IMO Video Meteor Network. The 2013 data were omitted from the average profile, since significantly enhanced activity that year would distort the profile.

[1]Abenstalstr. 13b, 84072 Seysdorf, Germany.
Email: sirko@molau.de
[2]Via Bobbio 9a/18, 16137 Genova, Italy.
Email: stefano.crivello@libero.it
[3]Urbanizacao da Boavista, Lote 46, Linhaceira, 2305-114 Asseiceira, Tomar, Portugal. Email: rui.goncalves@ipt.pt
[4]Rua Aquilino Ribeiro, 23 - 1 Dto. 2790028 Carnaxide, Portugal. Email: carlos.saraiva@netcabo.pt
[5]via Umbria 21/d, 30037 Scorze (VE), Italy.
Email: stom@iol.it
[6]Na Ajdov hrib 24, 2310 Slovenska Bistrica, Slovenia.
Email: javor.kac@orion-drustvo.si

IMO bibcode WGN-452-molau-vidnov
NASA-ADS bibcode 2017JIMO...45...43M

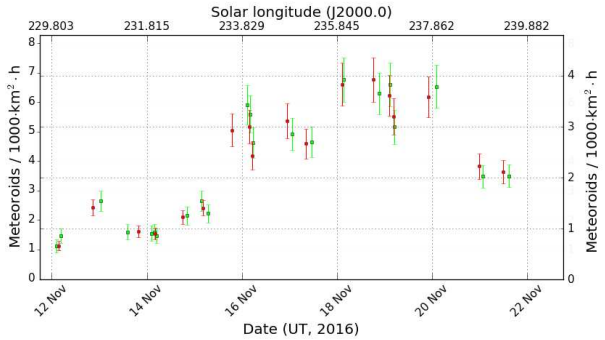

Figure 3 – Comparison of the 2016 Leonid flux density profile obtained with the previous (red, left axis) and new method (green, right axis) to calculate the limiting magnitude loss caused by meteor motion.

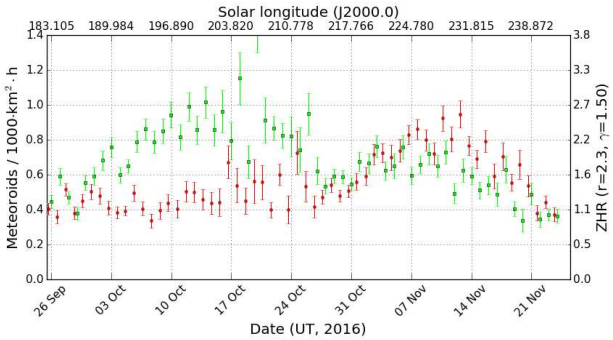

Figure 5 – Flux density of the Northern (red) and Southern Taurids (green) 2016, derived from video data of the IMO Video Meteor Network.

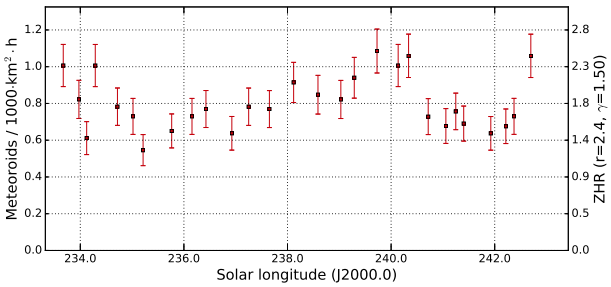

Figure 4 – Average activity profile of the α-Monocerotids from the years 2011–2016, derived from video data of the IMO Video Meteor Network.

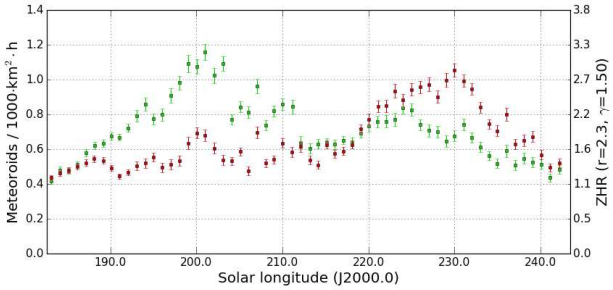

Figure 6 – Comparison of the average flux density profile of the Northern (red) and Southern Taurids (green) in the years 2011–2016. The 2015 data were omitted, since Taurid activity was enhanced that year by the "Taurid swarm".

3 α-Monocerotids

The α-Monocerotids also provided no surprises for observers. As in the previous few years they were effectively absent. Due to the small data set, we present in Figure 4 the average activity profile for the years 2011 to 2016.

4 Taurids

Figure 5 presents the flux density profile of the Northern and Southern Taurids. It seems remarkable that the Southern Taurids show maxima in mid-October and mid-November with a dip in-between. Since Northern Taurid activity also rises around the time of the second peak, we might suspect that once more we see the imprint of the lunar phase.

However, if all data from 2011 to 2016 are averaged (Figure 6) and only the 2015 data set is omitted (because of higher rates during the "Taurid swarm" that year), we get the same picture. The southern branch dominates in October and has a weak secondary peak in mid-November. The northern branch, on the other hand, is not very strong in October, but becomes quite prominent in November. The dip at the end of October is a real feature independent of the lunar phase.

References

Rendtel J. (2015). "2016 Meteor Shower Calendar". International Meteor Organization. IMO INFO(2-15).

Handling Editor: Javor Kac

Code	Name	Location	Camera	FOV [°2]	Stellar LM [mag]	Eff.CA [km^2]	Nights	Time [h]	Meteors
ARLRA	Arlt	Ludwigsfelde/DE	Ludwig2 (0.8/8)	1475	6.2	3779	24	165.4	949
BANPE	Bánfalvi	Zalaegerszeg/HU	Huvcse01 (0.95/5)	2423	3.4	361	14	55.0	122
BERER	Berkó	Ludányhalászi/HU	Hulud1 (0.8/3.8)	5542	4.8	3847	12	115.9	685
BOMMA	Bombardini	Faenza/IT	Mario (1.2/4.0)	5794	3.3	739	23	137.1	782
BREMA	Breukers	Hengelo/NL	Mbb3 (0.75/6)	2399	4.2	699	23	139.0	373
BRIBE	Klemt	Herne/DE	Hermine (0.8/6)	2374	4.2	678	19	100.3	456
		Bergisch Gladbach/DE	Klemoi (0.8/6)	2286	4.6	1080	19	102.9	423
CARMA	Carli	Monte Baldo/IT	Bmh2 (1.5/4.5)*	4243	3.0	371	3	24.4	63
CASFL	Castellani	Monte Baldo/IT	Bmh1 (0.8/6)	2350	5.0	1611	22	176.0	698
CRIST	Crivello	Valbrevenna/IT	Bilbo (0.8/3.8)	5458	4.2	1772	21	156.2	661
			C3P8 (0.8/3.8)	5455	4.2	1586	19	119.0	493
			Stg38 (0.8/3.8)	5614	4.4	2007	22	178.5	1289
DONJE	Donani	Faenza/IT	Jenni (1.2/4)	5886	3.9	1222	23	149.7	831
ELTMA	Eltri	Venezia/IT	Met38 (0.8/3.8)	5631	4.3	2151	14	97.5	451
FORKE	Förster	Carlsfeld/DE	Akm3 (0.75/6)	2375	5.1	2154	14	89.5	367
GONRU	Goncalves	Foz do Arelho/PT	Farelho1 (1.0/2.6)	6328	2.8	469	2	11.9	16
		Tomar/PT	Templar1 (0.8/6)	2179	5.3	1842	27	215.9	1043
			Templar2 (0.8/6)	2080	5.0	1508	26	220.2	838
			Templar3 (0.8/8)	1438	4.3	571	27	210.8	453
			Templar4 (0.8/3.8)	4475	3.0	442	27	199.0	801
			Templar5 (0.75/6)	2312	5.0	2259	27	196.8	980
GOVMI	Govedič	Središče ob Dravi/SI	Orion2 (0.8/8)	1447	5.5	1841	21	170.5	548
			Orion4 (0.95/5)	2662	4.3	1043	21	169.2	386
HERCA	Hergenrother	Tucson/US	Salsa3 (0.8/3.8)	2336	4.1	544	29	269.8	844
HINWO	Hinz	Schwarzenberg/DE	Hinwo1 (0.75/6)	2291	5.1	1819	1	10.4	40
IGAAN	Igaz	Hódmezővásárhely/HU	Huhod (0.8/3.8)	5502	3.4	764	21	145.9	393
		Budapest/HU	Hupol (1.2/4)	3790	3.3	475	2	7.6	11
JONKA	Jonas	Budapest/HU	Husor (0.95/4)	2286	3.9	445	20	155.0	325
			Husor2 (0.95/3.5)	2465	3.9	715	22	173.8	307
KACJA	Kac	Ljubljana/SI	Orion1 (0.8/8)	1399	3.8	268	12	45.3	88
		Kamnik/SI	Cvetka (0.8/3.8)*	4914	4.3	1842	11	67.6	415
			Rezika (0.8/6)	2270	4.4	840	11	72.3	769
			Stefka (0.8/3.8)	5471	2.8	379	11	72.8	310
		Kostanjevec/SI	Metka (0.8/12)*	715	6.4	640	3	22.8	65
KOSDE	Koschny	Izana Obs./ES	Icc7 (0.85/25)*	714	5.9	1464	25	176.1	1359
			Lic1 (2.8/50)*	2255	6.2	5670	27	216.8	1871
		La Palma/ES	Icc9 (0.85/25)*	683	6.7	2951	25	156.8	1361
			Lic2 (3.2/50)*	2199	6.5	7512	25	201.0	1748
LOPAL	Lopes	Lisbon/PT	Naso1 (0.75/6)	2377	3.8	506	3	3.5	24

Table 1 – Observers contributing to 2016 November data of the IMO Video Meteor Network. Eff.CA designates the effective collection area; the overall number of nights is the number of nights with at least one camera operating, the overall observing time and number of meteors are sums over all cameras.

Table 1 – Observers contributing to 2016 November data of the IMO Video Meteor Network – continued from previous page.

Code	Name	Location	Camera	FOV [°²]	Stellar LM [mag]	Eff.CA [km²]	Nights	Time [h]	Meteors
MACMA	Maciejewski	Chełm/PL	Pav35 (0.8/3.8)	5495	4.0	1584	12	47.3	118
			Pav36 (0.8/3.8)*	5668	4.0	1573	16	73.5	199
			Pav43 (0.75/4.5)*	3132	3.1	319	10	28.5	98
			Pav60 (0.75/4.5)	2250	3.1	281	16	80.9	281
MARGR	Maravelias	Lofoupoli-Crete/GR	Loomecon (0.8/12)	738	6.3	2698	12	94.7	192
MARRU	Marques	Lisbon/PT	Cab1 (0.75/6)	2362	4.8	1517	28	223.5	973
			Ran1 (1.4/4.5)	4405	4.0	1241	23	181.2	680
MASMI	Maslov	Novosibirsk/RU	Nowatec (0.8/3.8)	5574	3.6	773	3	26.6	133
MOLSI	Molau	Seysdorf/DE	Avis2 (1.4/50)*	1230	6.9	6152	20	144.7	1415
			Escimo2 (0.85/25)	155	8.1	3415	19	138.0	466
			Mincam1 (0.8/8)	1477	4.9	1084	20	132.9	928
		Ketzür/DE	Remo1 (0.8/8)	1467	6.5	5491	26	169.1	1142
			Remo2 (0.8/8)	1478	6.4	4778	26	172.0	1006
			Remo3 (0.8/8)	1420	5.6	1967	26	188.9	760
			Remo4 (0.8/8)	1478	6.5	5358	16	87.7	548
MORJO	Morvai	Fülöpszállás/HU	Huful (1.4/5)	2522	3.5	532	18	157.0	345
MOSFA	Moschini	Rovereto/IT	Rover (1.4/4.5)	3896	4.2	1292	14	16.2	117
OTTMI	Otte	Pearl City/US	Orie1 (1.4/5.7)	3837	3.8	460	24	205.8	372
PERZS	Perkó	Becsehely/HU	Hubec (0.8/3.8)*	5498	2.9	460	23	64.1	503
ROTEC	Rothenberg	Berlin/DE	Armefa (0.8/6)	2366	4.5	911	19	147.5	283
SARAN	Saraiva	Carnaxide/PT	Ro1 (0.75/6)	2362	3.7	381	22	148.1	308
			Ro2 (0.75/6)	2381	3.8	459	26	174.8	572
			Ro3 (0.8/12)	710	5.2	619	26	182.3	736
			Ro4 (1.0/8)	1582	4.2	549	10	52.2	111
			Sofia (0.8/12)	738	5.3	907	22	116.5	347
SCALE	Scarpa	Alberoni/IT	Leo (1.2/4.5)*	4152	4.5	2052	16	97.2	224
SCHHA	Schremmer	Niederkrüchten/DE	Doraemon (0.8/3.8)	4900	3.0	409	21	103.6	359
SLAST	Slavec	Ljubljana/SI	Kayak1 (1.8/28)	563	6.2	1294	12	68.4	284
			Kayak2 (0.8/12)	741	5.5	920	8	55.9	35
STOEN	Stomeo	Scorze/IT	Min38 (0.8/3.8)	5566	4.8	3270	20	111.4	773
			Noa38 (0.8/3.8)	5609	4.2	1911	19	112.1	611
			Sco38 (0.8/3.8)	5598	4.8	3306	21	118.4	900
STRJO	Strunk	Herford/DE	Mincam2 (0.8/6)	2354	5.4	2751	22	146.0	823
			Mincam3 (0.8/6)	2338	5.5	3590	21	137.0	479
			Mincam4 (1.0/2.6)	9791	2.7	552	14	71.9	73
			Mincam5 (0.8/6)	2349	5.0	1896	20	132.3	419
			Mincam6 (0.8/6)	2395	5.1	2178	21	140.5	466
TEPIS	Tepliczky	Agostyán/HU	Huago (0.75/4.5)	2427	4.4	1036	17	141.4	319
			Humob (0.8/6)	2388	4.8	1607	23	181.5	571
TRIMI	Triglav	Velenje/SI	Sraka (0.8/6)*	2222	4.0	546	19	139.7	205
WEGWA	Wegrzyk	Nieznaszyn/PL	Pav78 (0.8/6)	2286	4.0	778	17	76.6	253
YRJIL	Yrjölä	Kuusankoski/FI	Finexcam (0.8/6)	2337	5.5	3574	3	10.2	36
* active field of view smaller than video frame						Overall	30	9 774.9	42 776

The International Meteor Organization

www.imo.net

Follow us on Facebook InternationalMeteorOrganization

Follow us on Twitter @IMOMeteors

Council

President: Cis Verbeeck,
Bogaertsheide 5, 2560 Kessel, Belgium.
e-mail: cis.verbeeck@scarlet.be

Vice-President: Jürgen Rendtel,
Eschenweg 16, D-14476 Marquardt, Germany.
tel. +49 33208 50753
e-mail: jrendtel@aip.de

Secretary-General: Robert Lunsford,
14884 Quail Valley Way, El Cajon,
CA 92021-2227, USA. tel. +1 619 755 7791
e-mail: lunro.imo.usa@cox.net

Treasurer: Marc Gyssens, Heerbaan 74,
B-2530 Boechout, Belgium.
e-mail: marc.gyssens@uhasselt.be
BIC: GEBABEBB
IBAN: BE30 0014 7327 5911
Bank transfer costs are always at your expense.

Other Council members:

Megan Argo, Jodrell Bank Centre for Astrophysics, Alan Turing building, University of Manchester, Oxford Road, Manchester, M13 9PL, UK.
e-mail: megan.argo@gmail.com

Geert Barentsen, NASA Ames Research Center, M/S 244-30, Moffett Field CA 94035, USA.
e-mail: hello@geert.io

Javor Kac (see details under WGN)

Detlef Koschny, Zeestraat 46,
NL-2211 XH Noordwijkerhout, Netherlands.
e-mail: detlef.koschny@esa.int

Masahiro Koseki, 4-3-5 Annaka, Annaka-shi,
Gunma-ken 379-0116, Japan.
e-mail: geh04301@nifty.ne.jp

Sirko Molau, Abenstalstraße 13b, D-84072 Seysdorf, Germany. e-mail: sirko@molau.de

Jean-Louis Rault, Société Astronomique de France, 16, rue de la Vallée, 91360 Epinay sur Orge, France. e-mail: f6agr@orange.fr

Paul Roggemans, Pijnboomstraat 25, 2800 Mechelen, Belgium, e-mail: paul.roggemans@gmail.com

Galina Ryabova, Res. Inst. of Appl. Math. & Mech., Tomsk State University, Lenin pr. 36, build. 27, 634050 Tomsk, Russian Federation.
e-mail: ryabova@niipmm.tsu.ru

Damir Šegon, J. Rakovca 3, 52100 Pula, Croatia. e-mail: damir.segon@pu.t-com.hr

Juraj Tóth, Fac. Math., Phys. & Inf., Comenius Univ., Mlynska dolina, 84248 Bratislava, Slovakia.
e-mail: toth@fmph.uniba.sk

Commission Directors

Visual Commission: Rainer Arlt (rarlt@aip.de)
Generic e-mail address: visual@imo.net
Electronic visual report form:
http://www.imo.net/visual/report/electronic

Video Commission: Sirko Molau (video@imo.net)

Photographic Commission: Bill Ward (William.Ward@glasgow.ac.uk)
Generic e-mail address: photo@imo.net

Radio Commission: Jean-Louis Rault (radio@imo.net)

Fireballs: Online fireball reports:
http://fireballs.imo.net

Outreach Officer

Jure Atanackov, e-mail: jureatanackov@gmail.com

Press Officer

Megan Argo, e-mail: megan.argo@gmail.com

Webmaster

Karl Antier, e-mail: webmaster@imo.net

WGN

Editor-in-chief: Javor Kac
Na Ajdov hrib 24, SI-2310 Slovenska Bistrica, Slovenia. e-mail: wgn@imo.net;
include METEOR in the e-mail subject line

Editorial board: Ž. Andreić, M. Argo, D.J. Asher, F. Bettonvil, J. Correira, M. Gyssens, C. Hergenrother, T. Heywood, J. Rendtel, J.-L. Rault, C. Verbeeck, D. Vida, S. de Vet.

IMO Sales

Available from the Treasurer or the Electronic Shop on the IMO Website	€	$
IMO membership, including subscription to WGN Vol. 45 (2017)		
Surface mail	26	35
Air Mail (outside Europe only)	49	65
Electronic subscription only	21	25
Proceedings of the International Meteor Conference on paper		
1990, 1991, 1993, 1995, 1996, 1999, 2000, 2002, 2003, per year	9	12
2007, 2010, 2011, per year	15	20
2012, 2013, 2014, 2015 per year	25	34
2016	30	40
Proceedings of the Meteor Orbit Determination Workshop 2006	15	20
Radio Meteor School Proceedings 2005	15	20
Handbook for Meteor Observers	15	20
Meteor Shower Workbook	12	16
Electronic media		
Meteor Beliefs Project ZIP archive	6	8

Fireball on 2016 September 9 at $21^{\mathrm{h}}57^{\mathrm{m}}37^{\mathrm{s}}$ UT from Slovenia

This bright fireball of estimated magnitude -8 appeared over Slovenia on 2016 September 9, at $23^{\mathrm{h}}57^{\mathrm{m}}37^{\mathrm{s}}$ UT and was recorded by three meteor video cameras and six all-sky cameras in Slovenia.

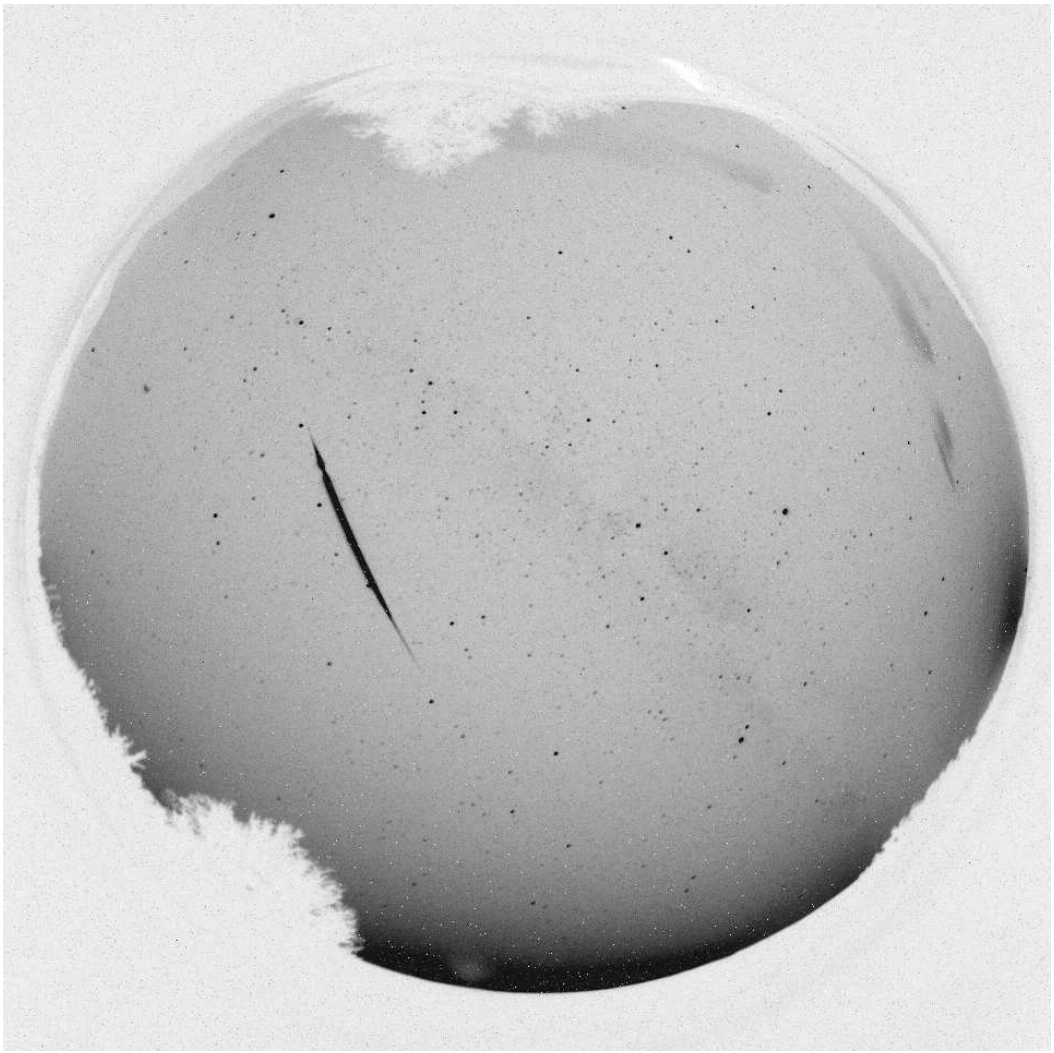

All-sky image captured from Rezman Observatory, Slovenia. The fireball was captured on two consecutive exposures of 30 s duration. Image courtesy: Javor Kac.

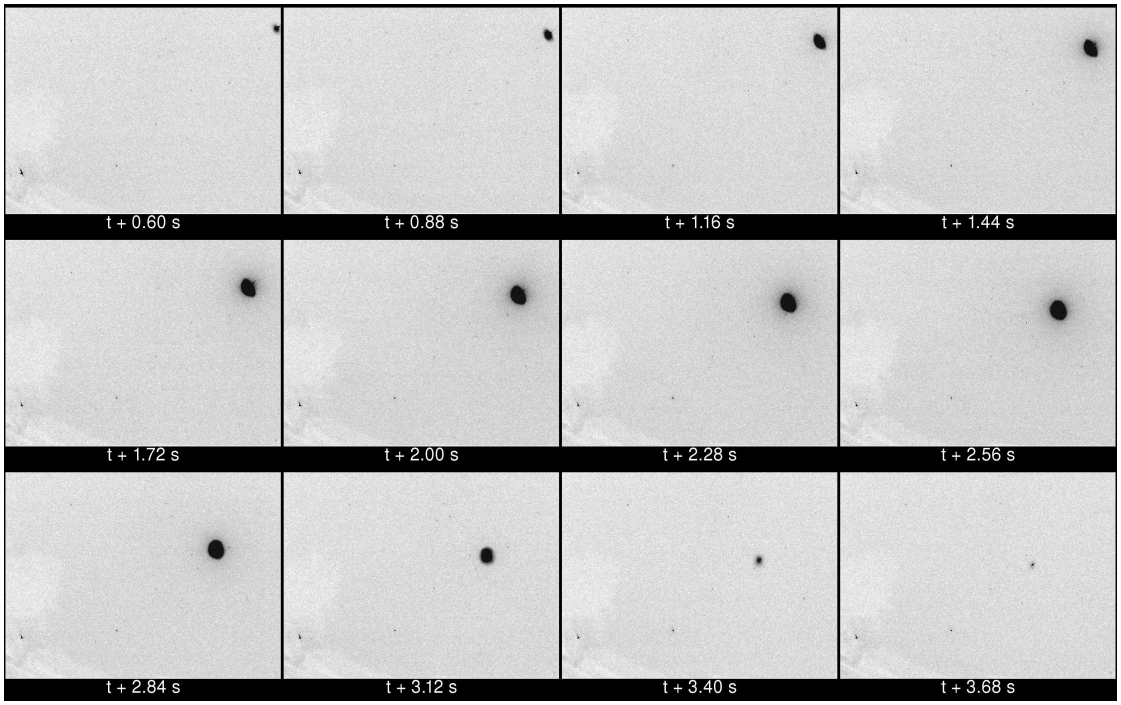

Still frames from video recording made by Cvetka camera stationed at Rezman Observatory, Slovenia, using 3.8-mm $f/0.8$ lens. Frames are marked with time since the beginning of the fireball. Image courtesy: Javor Kac.